Discussion Paper

Below the zero lower bound –
a shadow-rate term structure model
for the euro area

Wolfgang Lemke
(European Central Bank)

Andreea L. Vladu
(Deutsche Bundesbank and Johann Wolfgang Goethe University)

Non-technical summary

Research Question

In June 2014, the Governing Council of the ECB decided to decrease the deposit facility rate, one of its key policy rates, from zero to -10 basis points. Another rate cut to -20 basis points followed in September. Swap and bond yields of short- to medium-term maturities eventually turned negative as well. The removal of the zero lower bound raises the question of how to analyze the driving forces and exploit the information content of the yield curve in an unprecedented negative-rate environment.

Contribution

We develop an econometric model to analyse the euro-area yield curve from 1999 to mid-2015. The model belongs to the class of arbitrage-free 'shadow-rate' term structure models, which feature a lower bound on interest rates at any point in time. In contrast to most of the literature, which typically embodies a fixed lower bound of (slightly above) zero, our model caters for the possibility of an occasionally changing and possibly negative effective lower bound. We analytically inspect the mechanism by which such a change in the bound affects the yield curve. In contrast to most of the related studies, we use survey information to cross-check our results.

Results

We find that the market perception of the effective lower bound on euro-area interest rates decreased from marginally above zero to -11 basis points in September 2014. We argue that the lower bound itself can be interpreted as a 'monetary policy parameter' and illustrate that the decrease of the short end of the yield curve following the September 2014 ECB rate cut can be largely attributed to a decline in the lower bound. The model's forecasts are far more closely in line with corresponding survey forecasts and capture the decline in yield volatility far better than a popular benchmark model that ignores the presence of a lower bound. We estimate that since mid-2012, the median horizon after which future short rates are once again expected to exceed the level of 25 basis points has ranged between 18 and 62 months. Finally, we emphasize that quantifying this period is highly dependent on the estimated level of the lower bound, with a similar sensitivity also being evident when disentangling the expectations and term premia components embedded in bond yields.

Nichttechnische Zusammenfassung

Fragestellung

Im Juni 2014 entschied der EZB-Rat, den Zinssatz für die Einlagefazilität, einen der geldpolitischen Leitzinsen, von null auf -10 Basispunkte zu senken. Eine weitere Zinssenkung auf -20 Basispunkte folgte im September. Zinssätze von Swaps und Anleihen für kurze und mittlere Laufzeiten sanken schließlich ebenfalls in den negativen Bereich. Nach der Aufhebung der 'Null-Prozent Untergrenze' stellt sich die Frage, wie man in einem so noch nicht beobachteten Negativzinsumfeld die Bestimmungsfaktoren der Zinsstrukturkurve analysieren und ihren Informationsgehalt nutzen kann.

Beitrag

Wir entwickeln ein ökonometrisches Modell zur Analyse der Zinsstruktur im Euroraum für die Zeit von 1999 bis Mitte 2015. Das Modell gehört zur Klasse der arbitragefreien 'Schattenzins'- Zinsstrukturmodelle, die zu jedem Zeitpunkt eine Untergrenze vorsehen, die die Zinsen nicht unterschreiten können. Anders als im Großteil der bestehenden Literatur, bei dem typischerweise eine feste Zinsuntergrenze von (etwas über) Null angenommen wird, besteht in unserem Modell die Möglichkeit, dass sich die Zinsuntergrenze bisweilen ändert und negativ wird. Wir analysieren den Mechanismus, über den sich eine solche Änderung auf die Zinsstruktur auswirkt. Anders als die meisten anderen Studien ziehen wir Informationen aus Umfragen heran, um unsere empirischen Ergebnisse zu validieren.

Ergebnisse

Es zeigt sich, dass sich die effektive Zinsuntergrenze in der Wahrnehmung der Marktteilnehmer von zunächst knapp über Null im September 2014 auf -11 Basispunkte verringert hat. Wir erörtern, dass die Zinsuntergrenze selbst als 'geldpolitischer Parameter' interpretiert werden kann. Der Rückgang des kurzen Endes der Zinsstrukturkurve im September 2014 ist maßgeblich auf dieses Absinken der Untergrenze zurückzuführen. Modellprognosen des Kurzfristzinses stehen wesentlich besser im Einklang mit entsprechenden aus Umfragen abgeleiteten Prognosen als es für ein populäres Vergleichsmodell, das keine Zinsuntergrenze berücksichtigt, der Fall ist. Der mittlere Zeitraum, über den erwartet wird, dass Zinsen wieder über ein Niveau von 25 Basispunkten steigen, hat sich nach unseren Schätzungen seit Mitte 2012 zwischen 18 und 62 Monaten bewegt. Wir zeigen aber auch, dass die Quantifizierung dieses Zeitraums sehr stark vom geschätzten Niveau der Zinsuntergrenze abhängt. Eine vergleichbare Sensitivität der Ergebnisse gilt auch für die Zerlegung von Zinsen in Erwartungs- und Prämienkomponenten.

Below the Zero Lower Bound - A Shadow-Rate Term Structure Model for the Euro Area[*]

Wolfgang Lemke[†]   Andreea Liliana Vladu[‡]

Abstract

We propose an arbitrage-free shadow-rate term structure model to analyze the euro-area yield curve from 1999 to mid-2015, when bond yields turned negative at various maturities. In the model the 'shadow rate' can reach any positive or negative level, while the actual one-month rate cannot fall below some lower bound perceived by market participants. This bound is estimated to have first ranged marginally above zero, before falling to -11 bps in September 2014. We show analytically that the lower bound itself can be interpreted as a 'policy parameter' and interpret the September 2014 ECB rate cut from this perspective. Our model improves upon a standard Gaussian affine model by providing a better match with survey forecasts of short-term rates during the low-rate period and by capturing the decline in yield volatility. The model implies that since mid-2012, the median horizon after which future short rates are expected to return to 25 bps has ranged between 18 and 62 months. However, the liftoff timing, as well as the quantification of forward premia, is highly sensitive to the level of the lower bound.

Keywords: term structure of interest rates, lower bound, nonlinear state-space model, monetary policy expectations

JEL classification: C32, E43, E52

[†]European Central Bank, Sonnemannstr. 20, D-60314 Frankfurt am Main, Germany, wolfgang.lemke@ecb.int, corresponding author.

[‡]Deutsche Bundesbank and Johann Wolfgang Goethe University, Frankfurt am Main, Germany, andreea.liliana.vladu@bundesbank.de.

1 Introduction

Economists have traditionally assumed that nominal interest rates cannot fall below zero. The reasoning underlying the 'Zero Lower Bound' (ZLB) assumption is that investors would never hold a fixed-income instrument with a risk-free negative return, as holding cash – with a zero nominal return – would always be a superior alternative. Likewise, central banks were expected to be constrained by the ZLB when setting monetary policy rates in order to stimulate the economy in times of large economic slack and low, or even negative, inflation rates.[1]

When short rates reach the ZLB, they are typically observed to stick to the bound for some time, i.e. exhibiting exceptionally low volatility. At the same time, long rates would still move around, reflecting changing expectations about the timing of liftoff from the ZLB, the expected future path of policy rates after liftoff, as well as term premia. The popular class of Gaussian arbitrage-free affine term structure models (ATSMs) fails to account for the specific behavior of the yield curve near the ZLB, as rates in these models can become arbitrarily negative. Moreover, they have difficulty capturing the 'sticking' property of short-term rates at the ZLB, and instead tend to inadequately prescribe fast reversion to the long-run mean, which in turn biases the quantification of term premia.[2]

Accordingly, alternatives to the ATSM have been proposed to incorporate the ZLB restriction, among which the so-called shadow-rate term structure models (SRTSMs) have gained particular prominence.[3] These models incorporate linear Gaussian factor dynamics as driving forces – exactly as in Gaussian ATSMs – but it is the 'shadow short rate' s_t rather than the actual short-term rate r_t which is driven by those factors. The actual short rate is given as $r_t = max\{s_t, LB\}$: that is, it equals the shadow rate, if this is above the lower bound LB, while the actual short rate remains at the bound if the shadow rate is below the bound.[4]

However, the assumption of a *zero* (or slightly positive) lower bound has eventually become inadequate for several jurisdictions, as their central banks have taken recourse to negative policy rates. Examples include Denmark, Switzerland and – the focus of this paper – the euro area. In June 2014, the Governing Council of the European Central

---

[1]It has been acknowledged that the exact bound may actually be somewhat below zero if there are costs associated with holding cash or if bonds provide additional benefits to their holders apart from their direct pecuniary returns, see, e.g., the review by Yates (2004). However, the bulk of academic economic studies as well as central bank communication has taken the *zero* lower bound assumption as given and has instead focused on what other instruments are available to provide accommodation when short-term policy rates are constrained by the ZLB.

[2]See, e.g., Kim and Singleton (2012).

[3]For alternative approaches to capture yield curve behavior near the ZLB, see, e.g., Kim and Singleton (2012) and Monfort, Pegoraro, Renne, and Roussellet (2015).

[4]The idea of term structure modeling using the shadow rate dates back to Black (1995), but the literature on SRTSMs has proliferated in recent years when bond yields approached zero in several industrialized economies. In Japan, the period of very low interest rates already began in the early 2000s; see Ichiue and Ueno (2007), Ichiue and Ueno (2006), Kim and Singleton (2012) and Christensen and Rudebusch (2015) for analyses of the Japanese yield curve. For the U.S., the effective Federal funds rate reached a level below 0.2 percent at the end of 2008 and stayed close to zero until December 2015; see Krippner (2013a), Krippner (2013b), Kim and Priebsch (2013), Christensen and Rudebusch (2016), Bauer and Rudebusch (2016), Wu and Xia (2016). The Bank of England hit the effective lower bound ('bank rate' at 0.5 percent) in early 2009; see Andreasen and Meldrum (2015b) and Carriero, Mouabbi, and Vangelista (2015).

Bank (ECB) decided to decrease the deposit facility (DF) rate, one of their three key interest rates, to -10 basis points, and it followed up with a further rate cut to -20 basis points three months later. The interbank overnight rate (EONIA) dipped into negative territory in August 2014, and EONIA-linked Overnight Index Swap (OIS) rates fell below zero as well at that time.

This suggests that for the euro area it is not only necessary to relax the ZLB assumption and replace it by a negative lower bound, but it is also necessary to account for a possible shift in the bound itself: while investors considered negative rates inconceivable in the euro area for a long time, it would seem they adapted their view of the lower bound when the ECB decreased policy rates to negative levels. Moreover, after the move to negative territory, further changes of the market's *perceived* lower bound location are conceivable as the market may adjust its view over time on how negative the central bank may go.[5]

Accordingly, the paper proposes a novel discrete-time shadow-rate term structure model for the euro area, where we allow the lower bound to be negative and to change over time. Unlike most other literature on SRTSMs, we deploy survey data to inform the model specification and to validate some of the empirical findings. We allow a change in the lower bound to take place at two points in time: in May 2014, when several surveys suggested that markets started anticipating the June policy rate cut to -10 bps; and in September 2014, when the ECB decreased the deposit facility rate further to -20 bps, which – according to surveys – came rather unexpectedly. Hence, the most flexible model specification allows for three different lower bound regimes (1999 to April 2014, May 2014 to August 2014, and September 2014 to June 2015). Our discrete-time model is estimated using monthly observations of OIS zero-coupon rates from 1999 to June 2015. Parameters, including the levels of the lower bound, are estimated by maximum likelihood based on the extended Kalman filter.

The literature on shadow-rate models for the euro area is still relatively scarce. Pericoli and Taboga (2015) and Damjanović and Masten (2016) analyze the usefulness of the shadow short rate as a stance indicator, assuming a zero lower bound for their models. To our knowledge, the only other paper featuring a time-varying lower bound for the euro area is Kortela (2016), who, in contrast to our set-up, focuses on a continuously changing lower bound. Outside the euro area, specifications with a changing bound are naturally rare. Exceptions are Christensen and Rudebusch (2016), who perform a real-time estimation of the U.S. lower bound parameter, and Ichiue and Ueno (2013), who allow for a deterministic shift in the lower bound parameter for Japan.

Our main findings can be summarized as follows:

First, our preferred SRTSM specification suggests that there has been one change in the lower bound, namely from almost zero (point estimate of 1 basis point until August 2014) to negative (-11 basis points as of September 2014). While the most flexible model specification (with three potential lower bound regimes) suggests a first small decrease in the lower bound between the first (1999 to April 2014) and the second (May 2014 to

---

[5]While we will associate the move to negative rates and the further rate decrease within negative territory with possible shifts of the lower bound, one may alternatively hypothesize that such rate decisions have removed the lower bound altogether. However, as we will argue below, survey evidence and the econometric results point to the fact that in our sample, the 'shift in the bound' assumption is more adequate than the 'removal of the lower bound' assumption.

August 2014) subperiod, this change is found to be not statistically significant. Intuitively, this is due to the fact that following the first ECB rate cut to negative in June 2014, the movement of market rates into negative territory was rather sluggish, so that the data do not reject keeping a slightly positive effective lower bound until August 2014. As of September 2014, though, upon the second ECB rate cut to negative levels, the results suggest a significant decrease in the bound parameter.

Second, the preferred SRTSM with shifting lower bound has a very good fit (standard deviation of the measurement error amounts to about 3 bps) and is preferred based on econometric arguments over several natural competitor models such as the ATSM, an SRTSM with a zero lower bound, an SRTSM with a fixed estimated lower bound, and an SRTSM where the ECB's deposit facility rates themselves serve as lower bounds.

Third, the SRTSM matches short-rate expectations from surveys during the low-rate period fairly well and clearly improves upon the ATSM benchmark. Specifically, as mentioned before, short-term rates have a tendency to 'stick' to the lower bound once it has been reached. This is also reflected by predictions from the ECB Survey of Professional Forecasters (SPF), which likewise typically foresee a flat evolution of the short rate for several quarters ahead, once the short rate is at very low levels. This 'sticking property' can be well captured by the SRTSM, while the ATSM fails to account for that feature as it exhibits stronger reversion to the long-run mean of the short rate over medium horizons. At the same time, over short horizons, the ATSM often implies implausibly negative expected short rates, again disregarding the 'sticking' property of short-term rates. Accordingly, the SRTSM manages to match survey forecasts much better than the ATSM. The biased and excessively volatile rate expectations implied by the ATSM lead in turn to implausible estimates of forward premia during the low-rate period, while the SRTSM leads to more reasonable magnitudes for such measures of risk compensation.

Fourth, we show that our preferred SRTSM matches the stylized fact that conditional bond yield volatility has decreased when interest rates have moved closer to the lower bound. This is another major advantage compared to the ATSM, as the latter is by construction (unconditionally and conditionally) homoscedastic, so it implies a maturity-dependent but time-invariant variance pattern. Our findings for the euro area complement the literature that has documented this volatility feature of shadow-rate models for Japan; see Kim and Singleton (2012) and Christensen and Rudebusch (2015), and for the U.S.; see Christensen and Rudebusch (2016).

Fifth, we use the SRTSM for capturing the market-implied timing of when the short rate will lift off from the lower bound. Specifically, we quantify at each month the median timing at which the short rate will again exceed a threshold of 25 bps. The preferred specification implies that since mid-2012, this median crossing time has ranged between 18 and 62 months. Next, we document that different specifications of the lower bound (as described above) imply different crossing time estimates, which can hugely differ (by up to 48 months) from those implied by the preferred model. This feature differs notably from what is found in Krippner (2015), who shows that for the U.S. different lower bound specifications may imply different estimates of the shadow rates, but still fairly similar estimates of the liftoff time. Furthermore, we contribute to the literature by analyzing in detail how liftoff estimates can be biased when ignoring the presence of premia or the asymmetry of interest rates near the lower bound.

Finally, as a novelty in the literature, we analytically explore how a drop in the

perceived lower bound affects the term structure of interest rates.[6] For a given lower bound, the conditional distribution of future short rates is a censored normal with discrete probability mass at the lower bound and a normal density part governing the odds of rate realizations above the bound. A decrease in the lower bound parameter leads to assigning positive probabilities to rate realizations that had been infeasible under the old lower bound. This leads, ceteris paribus, to a decrease in expected rates, forward rates and spot rates. The strength of the effect is stronger, the closer forward and spot rates were ranging to the lower bound before its shift. Overall, these results have an important implication for monetary policy: if the central bank manages to decrease the market's perceived location of the lower bound, it can thereby decrease forward and spot rates, even in a situation where the lower bound is not yet binding. We apply the model to interpret the yield curve response to the ECB rate cut in September 2014. It turns out that for short maturities, the yield curve shift can to a large extent be explained through a drop in the lower bound, while for longer maturities a change in risk factors is needed to explain the remainder of the variation.

The paper is structured as follows. Section 2 describes the data and takes stock of some stylized facts of the euro-area yield curve. Section 3 introduces the model and the estimation approach. Section 4 covers the estimation results, including the goodness of fit regarding first and second moments, the matching of survey forecasts and forward premia. Section 5 is devoted to the analysis of liftoff timing. Section 6 elaborates on the effects of a change in the lower bound and applies such comparative statics to interpret the September 2014 shift in the euro-area yield curve.

2 Data and stylized facts

With our proposed model, we will analyze the dynamics of the term structure of 'risk-free' zero-coupon rates. Risk-free rates have generally been proxied by bond yields of highly-rated sovereign issuers, where zero-coupon rates for fixed maturities are usually extracted from the prices of coupon-bearing bonds.[7] However, for the euro area since 1999 there has not been a large issuer of high-rated euro-denominated public debt at the European (as opposed to the national) level. This problem is commonly circumvented by resorting to government bond yields of one single euro-area country, such as Germany, or by using synthetic yields extracted from a pool of several high-rated sovereign issuers. One problem with relying on German data is that during the global financial crisis and the euro-area sovereign debt market crisis, German government bond yields fell considerably, owing to the safe-haven status of German Bunds. Such safe-haven flows have the potential to compress German yields below those levels that would purely reflect short-rate expectations and corresponding term premia. Using, alternatively, synthetic yields based on all AAA-rated issuers suffers from similar shortcomings but is additionally challenged by the fact that the pool of AAA sovereigns can change and has in fact shrank during the sovereign debt crisis.

Therefore, the yield measures chosen in this paper are not based on bonds, but instead

---

[6]Kortela (2016) also focuses on the same matter but refers in turn to an earlier draft of our paper, see https://www.ecb.europa.eu/events/pdf/conferences/140908/lemke_vladu.pdf.

[7]See, e.g., BIS (2005) on the construction of zero-coupon curves.

rely on overnight index swap (OIS) rates based on EONIA, which is the overnight unsecured interbank rate in the euro area. OIS rates are increasingly considered as adequate proxies for risk-free rates, see, e.g., ECB (2014a). The market for these swap contracts started developing rapidly with the introduction of the euro in 1999.[8] OIS market activity was first concentrated at short maturities, but it gradually became more liquid for longer maturities as well, and swap rates for the medium to long-term segment of the OIS curve started being quoted at relatively stable spreads below Euribor swap rates. However, these spreads became larger and more volatile with the onset of the money market tensions in summer 2007, which then eventually morphed into the global financial crisis.

As a reliable set of zero-coupon OIS rates for various maturities is only available as of July 2005, we extend our data set backwards by splicing the OIS data with spread-adjusted zero-coupon rates based on Euribor swaps.[9] Specifically, for the backward extension of our OIS data set, we first compute the average spreads between end-of-month OIS and same-maturity Euribor spot rates over the period July 2005 to June 2007, i.e. a period for which both types of rates are available and for which the spreads between them were relatively stable. We then subtract these average spreads from the Euribor spot rates series from January 1999 to June 2005 and treat the thus-constructed time series as a replacement for the non-existent OIS spot rates over this period.[10] While aware of the fact that the data set results from splicing two different data types, we will nevertheless – for simplicity – just refer to OIS rates in the following.

Our yield data set comprises end-of-month observations for eight maturities (three- and six-month, one-, two-, three-, five-, seven- and ten-year) from January 1999 to June 2015. That is, we have $T = 198$ monthly observations of $J = 8$ points of the term structure of 'risk-free' interest rates. Figure 1 shows the time series of our spot rates data for the three-month, one-year, five-year and ten-year maturity together with two of the ECB's key policy rates, the main refinancing operations (MRO) rate and the deposit facility (DF) rate. In July 2012, the ECB decreased its DF rate to zero, so in this sense the euro area reached the zero lower bound at that point. For the remainder of the paper, we will occasionally differentiate between the period of historically low rates that started at that time ('low-rate' period, from July 2012 to June 2015), and the period before ('pre-low-rate' period, January 1999 to June 2012). The separation of these two sub-samples is purely for illustrative purposes and it does not influence the model estimation described below.

During the low-rate period, both the level and the volatility of spot rates look distinctly different compared to previous years. First, the term structure decreased considerably at all maturities (see Figure 2) with the average ten-year rate reaching a level of 1.23 percent compared to an average rate of 4.05 percent for the period before, and the average slope (ten-year minus three-month rate) decreased from 1.5 to 1.18 percent. Second, during the

---

[8]See, e.g., ECB (2001), section 4.2.

[9]For the three-month maturity we use the three-month Euribor rate, while for maturities of six months or higher we use the six-month Euribor rate and swap contracts with this underlying rate. We use spot rates derived by Bloomberg from quoted swap rates with a bootstrapping-interpolation method that guarantees a smooth instantaneous forward rate curve.

[10]The spreads between July 2005 and June 2007 were low and fairly stable. For example, the average end-of-month spread between zero-coupon rates derived from Euribor rates and Euribor rate swaps and OIS was 4 bps for the six-month maturity, 12 bps for the two-year maturity and 12 bps for the ten-year maturity, while the standard deviation of these spreads was 1, 2, and 3 bps, respectively.
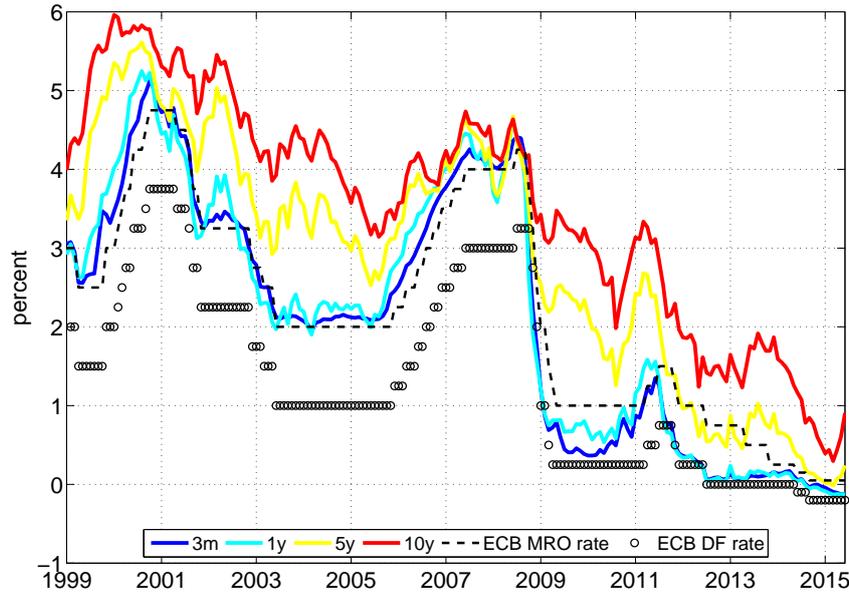
Figure 1: Euro-area interest rates since 1999.
Time-series of the three-month, one-year, five-year and ten-year euro-area zero-coupon OIS rates and the ECB's Main Refinancing Operation (MRO) and Deposit Facility (DF) rates. End-of-month realizations for January 1999 to June 2015.

low-rate period, realized volatilities (based on daily data)[11] of spot rates were distinctly lower compared to the previous period. As a case in point, the average annualized volatility of the one-year rate decreased from 52 to 16 bps. Similarly, long-term rates exhibited a decrease in average realized volatilities compared to the pre-low-rate period, see Figure 3.

In order to understand the behavior of the yield curve during the low-rate period, it is important to recognize that the ECB's DF rate provides a floor to EONIA, the overnight money market rate, and thereby to EONIA-based OIS rates. EONIA would not fall below the DF rate because it would not make sense for a bank to park liquidity overnight with another bank that pays an interest rate below the DF rate. Depending on the modus of monetary policy implementation and other factors, the distance between EONIA and the DF rate can be wider or smaller. As of 1999, EONIA initially ranged near the MRO rate and thus with a considerable distance to the DF rate, but with the inception of the ECB's 'fixed rate, full allotment' policy in October 2008, EONIA traded near the DF rate most of the time, rather than the MRO rate.[12] At the same time, the floor constituted by

---

[11]For each spot rate we compute the monthly realized volatility as the square root of the sum of the squared daily changes of the rate from that month. The daily data we use for this exercise is constructed in the same way as the end-of-month data set, i.e. a mix between spot rates derived from three- and six-month Euribor rates and Euribor swap rates until 30 June 2005 and OIS rates thereafter.

[12]The distance of EONIA and short-term OIS rates to the deposit facility rate depends, inter alia, on the level of excess liquidity and the extent of fragmentation in the interbank market, see, e.g. ECB (2014b), but their modeling is beyond the scope of the model class deployed in this paper.
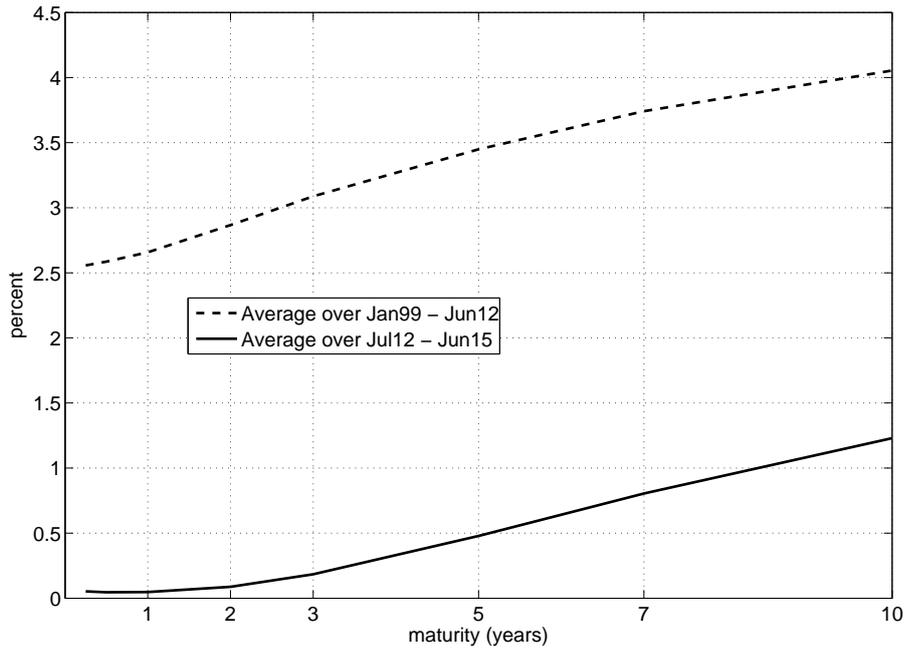
Figure 2: Average term structures across sub-samples in the euro area.
Average euro-area zero-coupon rates over two sub-samples: pre-low-rate period (January 1999 to June 2012) and low-rate period (July 2012 to June 2015).

the DF rate turned out to have almost never been binding. For instance, during the low-rate period, the three-month OIS rate ranged above the ECB's DF rate with an average distance of 12 bps (vs. 90 bps on average for the previous period). Hence, the upshot is that there needs to be a distinction between the *floor* for interest rates given by the DF rate and the *effective lower bound*, i.e. a level somewhat above the DF rate, around which short rates tended to fluctuate during the low-rate period. A similar distinction is acknowledged in the literature for the United States: while some studies have simply used zero as both the floor and the effective lower bound in their models, other studies have distinguished between the two concepts and have estimated or calibrated the effective bound at some margin above zero.[13]

What is special in the euro area is that the floor, and with it the effective lower bound, has itself apparently changed over time: while the DF rate had been zero for a time as of July 2012, it subsequently fell into negative territory, first to -10 bps in June and then further down to -20 bps in September 2014. After the June DF rate cut, short-term interest rates remained positive for a while, but on 25 August 2014, one-year and two-year

---

[13]Kim and Priebsch (2013) use end-of-month zero-coupon U.S. Treasury yields from January 1990 through June 2013 and estimate the lower bound at 14 bps. Christensen and Rudebusch (2016) derive a full-sample estimate of 11 bps with a similar data set expanding to October 2014. Wu and Xia (2016) set the U.S. lower bound at 25 bps, Akkaya, Gürkaynak, Kısacıkoğlu, and Wright (2015) choose a level of 10 bps, while Ichiue and Ueno (2013) set a level of 14 bps, which is the average value of the U.S. effective policy rates value from November 2009 to March 2013.
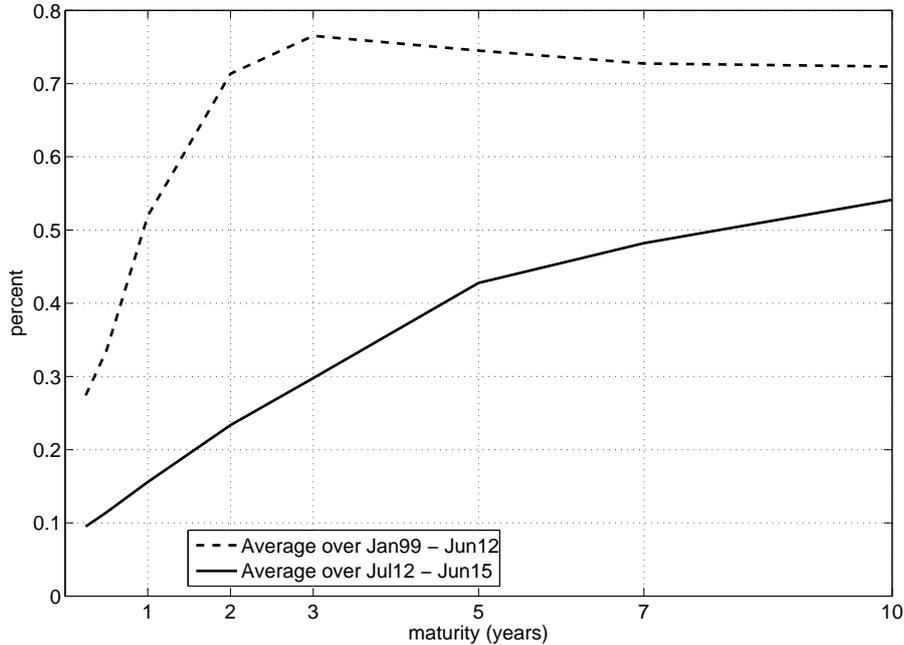
Figure 3: Average monthly term structures of realized volatilities in the euro area. Average monthly realized volatilities of euro-area zero-coupon rates for the pre-low-rate period (January 1999 to June 2012) and the low-rate period (July 2012 to June 2015), computed as the square root of the sum of squared daily changes of each rate within each month.

OIS rates eventually entered negative territory. EONIA itself went below zero for the first time on 28 August, while the three-month OIS rate followed on 1 September 2014. This suggests that we need our model of the euro-area term structure to account for a possible shift in the effective lower bound, which contrasts with the majority of studies for Japan, the United States or the UK that are based on a (assumed or estimated) fixed positive effective lower bound.

Ultimately, we will 'let the data decide' on the most plausible effective lower bound and how it has changed within our sample. However, an exploratory analysis of survey data already provides some indication of how market participants have adjusted their lower-bound perception over time.[14] Until April 2014, the majority of participants of a Bloomberg survey[15] did not foresee a cut to the DF rate for the next policy meeting;

---

[14]We cannot use surveys to infer the lower bound perceptions of individual participants *stricto sensu*, as we do not have individual forecasters' distributions but only their point forecasts. As a result, we can only get a first impression from surveys. However, we think that wherever the individual lower bounds of the panelists are located, a large degree of consensus in their point forecasts and their joint shift at a certain date would at least indicate that their lower bound perceptions may also have changed on this dates. Surveys may therefore help us spot the possible points in time at which we need to give the model at least the possibility to detect a change in the lower bound.

[15]Bloomberg asks market participants to provide their forecasts for the MRO and DF rate to be set in the next ECB monetary policy meeting. Answers are collected about one week before each meeting. The average number of respondents is 55 for the MRO rate question and 44 for the DF rate question.
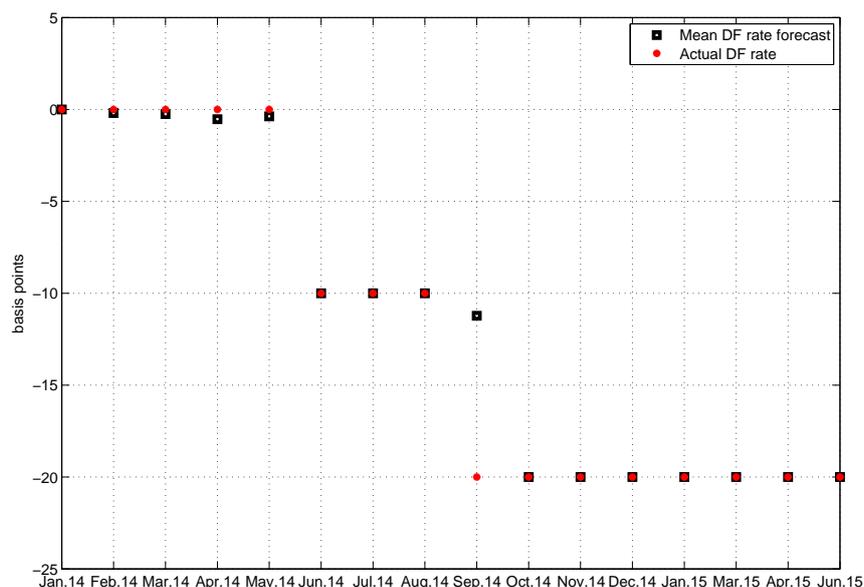
Figure 4: Bloomberg survey forecasts for the ECB DF rate and realizations.
Average survey forecasts for the deposit facility rate to be set at the ECB's next monetary policy meeting, together with the actual rates decided. Dates of the policy meetings are indicated on the x axis. The survey is conducted approximately one week before the actual meeting.

see Figure 4 and left panel of Figure 5. In other words, until that time, survey panelists appeared to be relatively certain about a zero floor for money market rates. This changed at the end of May 2014 when the majority of panelists did expect the ECB rate cut from June, including the drop of the DF rate from zero to negative; see Figure 5, middle panel. However, market participants did not seem to price in *further* rate cuts at that time, as evidence from a complementary survey collected by Reuters suggests.[16] In fact, the median forecast of future DF rates was -10 bps for horizons extending to 2015 Q4 in that survey. Overall, this suggests that market experts were assuming a floor of zero until April 2014; they then adapted their perception of that floor to a negative level, but did not expect a further downward shift in the future.

In fact, it would appear that the next ECB rate cut in September 2014 came unexpectedly to most survey participants, based on their predictions prior to the ECB's Governing Council meeting. At end-August, only 12% of Bloomberg survey participants envisaged a cut in the DF rate from -10 to -20 bps, while 88% were expecting rates to stay on hold; see Figure 5, right panel. Furthermore the Reuters survey collected on 28 August 2014 confirms that the September DF rate cut came largely as a surprise, as the

---

[16]We need to resort to the Reuters survey as well because, in contrast to the Bloomberg survey, it contains forecasts for horizons up to 1.5 years ahead, allowing us to assess market participants' expectations beyond the next ECB policy meeting. Unfortunately, we do not have access to answers at the individual forecaster level in the Reuters survey, but only to summary statistics and the number of respondents that anticipated policy rate increases or decreases. The two surveys are very similar in terms of average number of respondents.
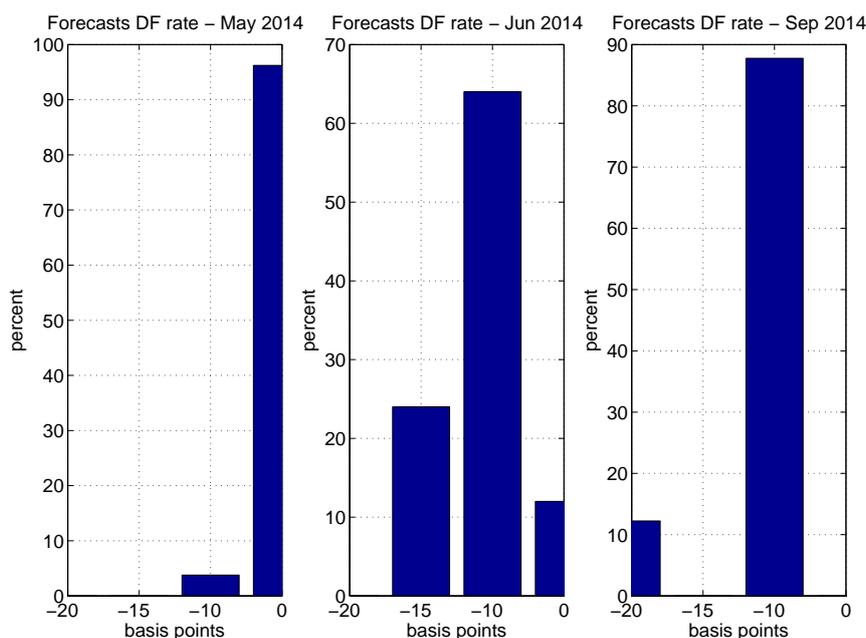
Figure 5: Histograms of Bloomberg survey forecasts for the ECB DF rate.
Distribution of survey forecasts for the ECB's next policy meeting decision for the DF rate for the meetings in May, June and September 2014. Each bar represents the percentage of respondents that provided as forecast for the DF rate the values indicated on the x axis. The actual DF rates decided for these dates are 0 bps (May 2014), -10 bps (June 2014), and -20 bps (September 2014).

median forecast saw the ECB sticking to a DF rate of -10 bps and only less than 7% of participants had forecast the September DF rate cut. Beyond this, no new rate cuts were envisaged by Reuters survey participants, based on their responses regarding the Governing Council's decision from October 2014: both the median and the minimum of their forecasts for the DF rate was -20 bps until 2016 Q1.

Summing up, survey evidence suggests two potential shifts in the floor (and correspondingly to the effective lower bound) of euro-area interest rates: in May 2014, when investors started pricing in (correctly) the first rate cut from zero to negative in the following month; and in September 2014, when the market observed the second – and largely unexpected – rate cut further into negative territory. Accordingly, we will allow for this non-standard feature of a shifting bound in our shadow rate model. Moreover, in order to keep the model tractable, we will implicitly deem that agents, when pricing bonds and swaps, assume the same lower-bound to prevail over the whole maturity of the respective instrument. Again, the data will eventually decide how adequate this assumption is for bond pricing, but the reported survey evidence hints that this may not be a too far-fetched assumption.

3 Model and estimation approach

We employ a latent-factor arbitrage-free term structure model in discrete time, with linear Gaussian factor dynamics and a nonlinear mapping between factors and the short-term (i.e. one-period) interest rate, which ensures that the short rate will not fall below a given lower bound. Under the condition of no-arbitrage, zero-coupon bond prices are risk-neutral expectations of the discounted payoff at maturity. Throughout, the periodicity is monthly, in line with our empirical set-up.

3.1 Model and approximation of zero-coupon bond yields

Specifically, under the risk-neutral probability measure $\mathbb{Q}$, $N = 3$ factors, $X = (X^1, X^2, X^3)'$, follow a first-order Gaussian VAR:

$$\Delta X_t = K_0^{\mathbb{Q}} + K_1^{\mathbb{Q}} X_{t-1} + \Sigma \epsilon_t^{\mathbb{Q}}, \quad \epsilon_t^{\mathbb{Q}} \overset{iid}{\sim} N(0, I_N). \tag{1}$$

The physical ('real-world') factor dynamics, i.e. under probability measure $\mathbb{P}$, are also given as a Gaussian VAR, but possibly with mean and persistence parameters different from their $\mathbb{Q}$-measure counterpart:

$$\Delta X_t = K_0^{\mathbb{P}} + K_1^{\mathbb{P}} X_{t-1} + \Sigma \epsilon_t^{\mathbb{P}}, \quad \epsilon_t^{\mathbb{P}} \overset{iid}{\sim} N(0, I_N). \tag{2}$$

The one-period 'shadow short rate' s_t is specified as an affine function of factors:

$$s_t = \rho_0 + \rho_1' X_t. \tag{3}$$

The actual observable short rate r_t is equal to the shadow short rate if the latter is above a lower bound LB, otherwise the short rate sticks to that bound; see left panel of Figure 6 for an illustration using a hypothetical lower bound of $LB = 0\%$.

$$r_t = \max\{s_t, LB\} \tag{4}$$

Linking the short rate to the shadow rate via (4) is a technical means to avoid the short rate reaching implausibly low levels. Moreover, if the shadow rate is sufficiently far below LB and the factors driving the shadow rate are fairly persistent, then the shadow rate is expected to stay below the bound for several periods in a row and, accordingly, the short rate is expected to stick to the lower bound during that time.

The Gaussian shadow-rate dynamics coupled with the bound specification (4) implies that the conditional distribution at time t of the short rate h periods ahead is censored: with positive probability the future short rate is realized at LB, and the remaining probability mass is distributed over realizations above the bound. See the right panel of Figure 6 for an illustration. More formally, the conditional density of the shadow rate h periods ahead $p_t(s_{t+h})$ is Gaussian, while the conditional distribution of the short rate r_{t+h} has a censored normal distribution with a point mass of $Prob_t(s_{t+h} \leq LB)$ at LB and a normal density part $p_t(s_{t+h})$ to the right of it. This type of distribution prevails for both $\mathbb{P}$ and $\mathbb{Q}$ probability measures.

Using the short-hand notation $\mu_{t,h} = E_t(s_{t+h})$ and $(\sigma_h)^2 = Var_t(s_{t+h})$, the conditional
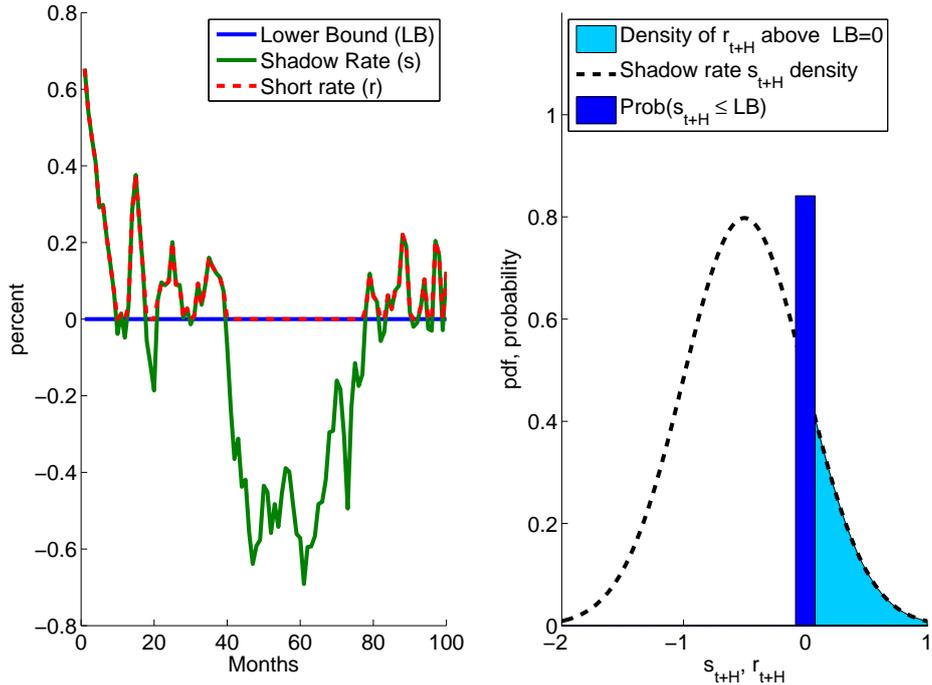
Figure 6: Illustration of relation between short rate and shadow short rate, and shape of short rate predictive distribution.
Typical time-series realizations of the short rate and the shadow short rate with zero lower bound (left panel), and a typical predictive distribution for the short rate, i.e. a censored normal distribution (right panel). Arbitrary parametrization for illustrative purposes, lower bound $LB = 0$ for both panels.

probability of the short rate sticking to the bound is given by $Prob_t(r_{t+h} = LB) = Prob_t(s_{t+h} \leq LB) = \Phi\left(\frac{LB - \mu_{t,h}}{\sigma_h}\right)$, where $\Phi(\cdot)$ is the standard normal cdf.[17] Using a standard result on the censored normal distribution,[18] the expected future short rate has a closed-form expression as

$$E_t(r_{t+h}) = LB + \sigma_h \cdot H\left(\frac{\mu_{t,h} - LB}{\sigma_h}\right), \tag{5}$$

where $H(x) = x\Phi(x) + \phi(x)$ and $\phi(\cdot)$ is the standard normal pdf.

From (5) it is easy to see that when $E_t(s_{t+h}) \gg LB$, i.e. the expected shadow rate is unlikely to undershoot the lower bound, then $H(x) \to x$ and $E_t(r_{t+h}) \approx E_t(s_{t+h})$, i.e. the expected short rate is close to the expected shadow rate. Conversely, when $E_t(s_{t+h}) \ll LB$, i.e. the expected shadow rate is far below the bound, then $H(x) \to 0$ and $E_t(r_{t+h}) \approx LB$, i.e. the short rate is expected to be stuck at the bound.

The price at time t of a zero-coupon bond that pays off one unit of account at time

---

[17]Note that due to the linear Gaussian factor dynamics, conditional expectations of the shadow short rate $\mu_{t,h}$ are time and horizon-dependent, while variances σ_h are only horizon-dependent but time-invariant.

[18]See, e.g,. Greene (1997).

$t + n$ is denoted by P_t^n. The family of arbitrage-free bond prices for all t and n is given by:

$$P_t^n = E_t^{\mathbb{Q}} \left[exp \left(- \sum_{i=0}^{n-1} r_{t+i} \right) \right]. \tag{6}$$

Bond yields for maturity n result from bond prices via $y_t^n = -\frac{1}{n} \ln P_t^n$.

Solving the model means finding a family of functions g_n, which for each maturity n maps factors into bond yields, given the parameters constituting the risk-neutral factor dynamics in (1) and the mapping between factors and the shadow rate (3) as well as the lower bound parameter LB:

$$y_t^n = g_n \left(X_t; K_0^{\mathbb{Q}}, K_1^{\mathbb{Q}}, \Sigma, \rho_0, \rho_1, LB \right). \tag{7}$$

Without the lower-bound constraint (4), we would be back to the Gaussian affine term structure model (ATSM), where the short rate r_t is affine in the latent factors:

$$r_t = \rho_0 + \rho_1' X_t. \tag{8}$$

This assumption, together with equations (1) and (6), leads to the yield function g_n being affine in factors in the ATSM model:

$$y_t^n = A_n + B_n' X_t, \tag{9}$$

where A_n and B_n solve the first order difference equations

$$\Delta B_n = K_1^{\mathbb{Q}'} B_{n-1} - \rho_1, \tag{10}$$

$$\Delta A_n = K_0^{\mathbb{Q}'} B_{n-1} + \frac{1}{2} B_{n-1}' \Sigma \Sigma' B_{n-1} - \rho_0, \tag{11}$$

with the initial conditions $A_0 = 0$ and $B_0 = 0$; see, e.g., Duffie and Kan (1996).

However, with a lower bound restriction in place, the function g_n that maps factors into bond yields is nonlinear. For the one-factor model ($N = 1$), g_n can be represented in closed form[19], but an exact analytical solution is not available for $N > 1$. Models with two factors ($N = 2$) already pose serious challenges for computing bond prices and in turn increase the computational burden for model estimation.[20] To overcome these challenges and estimate models with even three or four factors, the bulk of the recent literature employs option-based approximations to the yield functions; see Krippner (2012), Priebsch (2013), Christensen and Rudebusch (2015) for models in continuous time and Wu and Xia (2016) for their discrete time counterparts.[21]

---

[19]See Gorovoi and Linetsky (2004) for analytical solutions for zero-coupon bonds, as well as bond options, derived with the method of eigenfunction expansions.

[20]Ichiue and Ueno (2007) apply a lattice method, while Kim and Singleton (2012) and Bomfim (2003) employ finite-difference methods for computing bond prices.

[21]Regarding alternative approaches, Pericoli and Taboga (2015) use an exact Bayesian method of estimation with simulations, while Ueno, Baba, and Sakurai (2006) and Akkaya et al. (2015) apply Monte Carlo simulations to evaluate shadow-rate models for a given set of parameters. Andreasen and Meldrum (2015a) and Andreasen and Meldrum (2015b) deploy a sequential regression approach.

In this paper, we rely on the approximation introduced by Wu and Xia (2016). They show that the implied one-month forward rate h months ahead, f_t^h, can be approximated as

$$f_t^h \approx LB + \sigma_h^{\mathbb{Q}} \cdot H \left(\frac{\mu_{t,h}^{\mathbb{Q}} - LB - J_h}{\sigma_h^{\mathbb{Q}}} \right), \tag{12}$$

where $\mu_{t,h}^{\mathbb{Q}} = E_t^{\mathbb{Q}}(s_{t+h})$, $\left(\sigma_h^{\mathbb{Q}} \right)^2 = Var_t^{\mathbb{Q}}(s_{t+h})$, $H(x)$ is defined as above for (5), and J_h is a variance term, which depends on the horizon h but is independent of the factors and the lower bound. Note that this expression is the same as $E_t^{\mathbb{Q}}(r_{t+h})$ using (5), except for the term J_h, which is needed in the pricing formula approximation due to the fact that $E_t^{\mathbb{Q}}(r_{t+h})$ differs from f_t^h by a Jensen inequality term.

Using the identity that spot rates are averages of forward rates, we can approximate the function g_n in (7), mapping factors to yields, as

$$\begin{aligned}
y_t^n &\approx \tilde{g}_n \left(X_t; K_0^{\mathbb{Q}}, K_1^{\mathbb{Q}}, \Sigma, \rho_0, \rho_1, LB \right) \\
&= \frac{1}{n} \left[r_t + (n-1) LB + \sum_{h=1}^{n-1} \sigma_h^{\mathbb{Q}} \cdot H \left(\frac{\mu_{t,h}^{\mathbb{Q}} - LB - J_h}{\sigma_h^{\mathbb{Q}}} \right) \right].
\end{aligned} \tag{13}$$

For the parametrization of the SRTSM, we follow the normalization used in Joslin, Singleton, and Zhu (2011).[22] The autoregressive matrix under the $\mathbb{Q}$ measure is diagonal, $K_1^{\mathbb{Q}} = diag(K_{1,11}^{\mathbb{Q}}, K_{1,22}^{\mathbb{Q}}, K_{1,33}^{\mathbb{Q}})$, the intercept vector is $K_0^{\mathbb{Q}} = (K_{0,1}^{\mathbb{Q}}, 0, 0)'$, while the matrix Σ is lower triangular. Regarding the mapping from factors to the shadow rate, we assume $\rho_0 = 0$ and $\rho_1 = [1, 1, 1]$. For the $\mathbb{P}$ dynamics we assume that $K_0^{\mathbb{P}}$ and $K_1^{\mathbb{P}}$ are freely parametrized. The same normalization is also used for estimating the ATSM.

3.2   Estimation approach

As discussed in Section 2 above, the data appear to allow for a possible shift in the lower bound in May and September 2014. Hence, equation (4) will be modified by adding a time index to the lower bound LB, denoting that the empirical model takes this possibility into account:

$$r_t = \max \{ s_t, LB_t \}. \tag{14}$$

Specifically, consider subperiods A – January 1999 to April 2014, B – May 2014 to August 2014, and C – September 2014 to June 2015. The model is estimated assuming a fixed – but unknown – bound parameter for subperiod A, a potentially different bound for subperiod B, and possibly yet another bound parameter for subperiod C. All other parameters are assumed to be constant over the whole sample. Importantly, the changing bounds are implemented such that at any point in time t, bonds are priced as if the current bound would prevail with certainty into the indefinite future.[23] As argued in Section

---

[22]Bauer and Rudebusch (2016) use the same set of identifying restrictions.

[23]Our assumption is in line with the "anticipated utility approach" (see, e.g., Cogley and Sargent (2009)) which is used frequently in the asset pricing literature with time-varying parameters; see, e.g., Johannes, Lochstoer, and Mou (2016), Laubach, Tetlow, and Williams (2007) or Orphanides and Wei (2012). The upshot is that even if agents see the possibility of parameters changing in the future (here: that the lower bound may change in the future), they base their pricing decision on their *current* perception of parameters (here: their current best guess of the lower bound). A more sophisticated specification

2 above, survey evidence suggests that this may not be a too far-fetched assumption. Finally, our specification with potential shift in the lower bound obviously nests the more standard set-up with a constant (and possibly *zero*) lower bound for the full time sample ABC – January 1999 to June 2015, as well as the one with the same bound over the full subperiod AB – January 1999 to August 2014 – but possibly a different bound for subperiod C.

For estimation purposes, the SRTSM is cast into state-space form. The transition equation is given by the linear Gaussian factor dynamics under the $\mathbb{P}$ measure, (2),

$$X_t = K_0^{\mathbb{P}} + \left(I_N + K_1^{\mathbb{P}}\right) X_{t-1} + \Sigma \epsilon_t^{\mathbb{P}}, \quad \epsilon_t^{\mathbb{P}} \overset{iid}{\sim} N\left(0, I_N\right). \tag{15}$$

Denote by y_t^o the measurement vector $y_t^o = (y_t^{3m,o}, \dots, y_t^{10y,o})'$ of $J = 8$ yields (three- and six-month, one-, two-, three-, five-, seven- and ten-year, see Section 2) observed at time t. The measurement equation equates the observed data to their model-implied counterparts plus a measurement error. As usual, the measurement errors capture approximation errors in the sense that the data are not necessarily ideal representatives of risk-free zero-coupon yields, but they also serve as residuals in the broader sense of capturing all other deviations between model yields and data. For simplicity and parsimony, we assume that the measurement errors have the same variance across maturities:

$$\begin{pmatrix} y_t^{3m,o} \\ \vdots \\ y_t^{10y,o} \end{pmatrix} = \begin{pmatrix} \tilde{g}_{3m}\left(X_t; K_0^{\mathbb{Q}}, K_1^{\mathbb{Q}}, \Sigma, \rho_0, \rho_1, LB_t\right) \\ \vdots \\ \tilde{g}_{10y}\left(X_t; K_0^{\mathbb{Q}}, K_1^{\mathbb{Q}}, \Sigma, \rho_0, \rho_1, LB_t\right) \end{pmatrix} + \begin{pmatrix} \epsilon_t^{3m} \\ \vdots \\ \epsilon_t^{10y} \end{pmatrix}, \quad \epsilon_t^n \overset{iid}{\sim} N\left(0, \sigma_e^2\right), \tag{16}$$

with $\tilde{g}_n$ as in (13) above.

The parameters to be estimated are collected in the vector

$$\begin{aligned} \Psi \;=\; & \left(K_{0,1}^{\mathbb{Q}}, K_{1,11}^{\mathbb{Q}}, K_{1,22}^{\mathbb{Q}}, K_{1,33}^{\mathbb{Q}}, K_{0,1}^{\mathbb{P}}, K_{0,2}^{\mathbb{P}}, K_{0,3}^{\mathbb{P}}, K_{1,11}^{\mathbb{P}}, \right. \\ & \left. K_{1,12}^{\mathbb{P}}, \dots, K_{1,33}^{\mathbb{P}}, \Sigma_{11}, \Sigma_{21}, \dots, \Sigma_{33}, LB_A, LB_B, LB_C, \sigma_e \right), \end{aligned} \tag{17}$$

with a size of 26 elements (when the bound parameters for all three subperiods are mutually distinct).

Our state-space model features a linear transition equation but a nonlinear measurement equation. Following Kim and Singleton (2012), Christensen and Rudebusch (2015) and Krippner (2013a), we estimate the model by maximum likelihood, based on the extended Kalman filter.[24] The extended Kalman filter requires the Jacobian of the yield function (7) with respect to factors X_t. Based on the linear approximation for yields in (13), the Jacobian is approximated analytically.[25] Starting values for the SRTSM param-

eters Ψ (with the exception of LB_A, LB_B, and LB_C) are taken from the ATSM parameters, which are estimated by maximum likelihood based on the standard Kalman filter, following the approach in Joslin et al. (2011).

3.3 Transformation of factors in SRTSM and ATSM

So far, our representation of the SRTSM has been based on generic latent factors X_t with their dynamics restricted for econometric identification. However, for easier economic interpretation, we will also consider an equivalent representation with new latent factors $\mathcal{P}_t$ resulting from X_t via an affine transformation $\mathcal{P}_t = P_0 + P_1 X_t$, which makes the new factors (almost) resemble principal components, at least during the pre-low-rate period. We obtain specific values for P_0 and P_1 from the estimation of the ATSM along the lines of Joslin et al. (2011).[26] Next, we apply them to filtered SRTSM latent factors X_t to derive new latent SRTSM factors $\mathcal{P}_t$.

The starting point for the transformation used by Joslin et al. (2011) for simplifying the ATSM estimation is a loading matrix W that maps the set of our $J = 8$ observed yields y_t^o into the first three observable principal components

$$\mathcal{P}_t^o = W y_t^o. \tag{18}$$

Given initial guesses for restricted parameters governing the $\mathbb{Q}$-dynamics of factors X_t from (1), loadings A_n and B_n from (9) can be computed recursively and the vector of J ATSM-implied yields is given as $y_t = A + B X_t$. By applying the W matrix to these yields,

$$\mathcal{P}_t = W y_t = W (A + B X_t) = W A + W B X_t, \tag{19}$$

one constructs a new set of ATSM latent factors $\mathcal{P}_t$, that are an affine transformation of the latent factors X_t. Importantly, given the affine transformation from (19), ATSM yields can also be expressed as affine expressions of pricing factors $\mathcal{P}_t$:

$$y_t = A_\mathcal{P} + B_\mathcal{P}' \mathcal{P}_t, \tag{20}$$

where $A_\mathcal{P}$ and $B_\mathcal{P}$ are known given A and B.[27]

After estimating the SRTSM with identifying constraints on the factor dynamics as described in the previous subsection, we apply an affine transformation to the latent SRTSM factors X_t, thus constructing a new set of SRTSM latent pricing factors $\mathcal{P}_t$:

$$\mathcal{P}_t = W A + W B X_t, \tag{21}$$

where W is defined in (18), and A and B are defined in (19) and stem from the ATSM estimation (which we conduct before the SRTSM estimation). That is, both ATSM and

---

SRTSMs in discrete time.

[26] Joslin et al. (2011) show that choosing a specific transformation that leads in the ATSM to latent factors that resemble, with small deviations, the principal components of observed zero-coupon yields enormously facilitates the estimation of the model due to the very good starting values for some of the parameters that are otherwise very hard to pin down.

[27] From equation (19) it follows that $X_t = (WB)^{-1} (\mathcal{P}_t - WA)$. Plugging this expression in $y_t = A + B X_t$ and grouping terms leads to $A_\mathcal{P} = [I - B (WB)^{-1} W] A$ and $B_\mathcal{P} = B (WB)^{-1}$.

SRTSM are subject to the same factor rotation.

Given the estimated parameters Ψ, see (17), corresponding to the SRTSM representation in factors X_t, the dynamics of the transformed factors $\mathcal{P}_t$ have laws of motion as in (1) and (2), with corresponding parameters given by $K_{0,\mathcal{P}} = WBK_0 - WBK_1 (WB)^{-1} WA$ and $K_{1,\mathcal{P}} = WBK_1 (WB)^{-1}$, both for the $\mathbb{P}$ and $\mathbb{Q}$ dynamics, and variance-covariance matrix of innovations $\Sigma_{\mathcal{P}} \Sigma'_{\mathcal{P}} = WB\Sigma\Sigma' (WB)'$. The mapping from the transformed factors to the shadow rate is of the same form as (3), with the transformed parameters resulting from the original parameters as $\rho_{0,\mathcal{P}} = \rho_0 - \rho'_1 (WB)^{-1} WA$ and $\rho_{1,\mathcal{P}} = \left((WB)^{-1}\right)' \rho_1$.[28] The mapping (4) from the shadow rate into the short rate stays the same.

Proceeding in this way, factors $\mathcal{P}_t$ generate the same shadow short-rate dynamics and hence the same short-rate dynamics as under the original factors X_t, both under $\mathbb{P}$ and $\mathbb{Q}$. Accordingly, for any realization of X_t, i.e. the non-transformed factor vector, the transformed factors $\mathcal{P}_t$ generate the same set of zero-coupon yields and model-implied objects, such as forward curves, conditional yield volatility or forward premia.

4 Estimation results

4.1 Parameter estimates and the number of lower bound regimes

We estimate five different specifications of the SRTSM, which differ by the restrictions imposed on the lower bound parameters LB_A (the bound perceived to be prevailing between 1999 and April 2014), LB_B (the bound between May and August 2014), and LB_C (the bound between September 2014 and June 2015). The (estimated) lower bounds and corresponding likelihoods are reported in Table 1 in the Appendix.

First, the most flexible specification (SRTSM-3LB) leads to estimates of $\hat{LB}_A = 2$ bps, $\hat{LB}_B = 1$ bp and $\hat{LB}_C = -11$ bps. By construction, it exhibits the highest likelihood. As the estimated lower bounds for the first two sub-periods are very similar, the second specification (SRTSM-2LB) assumes $\hat{LB}_A = \hat{LB}_B =: \hat{LB}_{AB}$. In fact, a likelihood ratio test, see Table 2 in the Appendix, suggests that one cannot reject this coefficient restriction (p-value = 11.5%). Third, we consider a specification (SRTSM-3LB-DFR) that equates the lower bounds to the respective ECB's deposit facility rate, which constitutes the floor for EONIA at any point in time, i.e. $\hat{LB}_A = 0$ bps, $\hat{LB}_B = -10$ bps and $\hat{LB}_C = -20$ bps.[29] This coefficient restriction is clearly rejected by the data, indicating that the *effective* lower bound is located above these numbers. Fourth, the standard *zero* lower bound assumption (specification SRTSM-ZLB) also results in a markedly lower likelihood and is rejected by the likelihood ratio test. Fifth, for the SRTSM specification with only one estimated lower bound parameter (SRTSM-1LB), we obtain $\hat{LB}_A = \hat{LB}_B = \hat{LB}_C =: \hat{LB}_{ABC} = -10$ bps. This model has a higher likelihood than the SRTSM-ZLB, indicating that the data supports a negative rather than a zero effective lower bound. However, the specification with $\hat{LB}_{ABC} = -10$ bps is also clearly rejected in favor of the model SRTSM-2LB, where

---

[28]Parameters of ATSM latent factors $\mathcal{P}_t$ transformed as in (19) are constructed identically, with the sole exception that the transformed parameters $\rho_{0,\mathcal{P}}$ and $\rho_{1,\mathcal{P}}$ map $\mathcal{P}_t$ into the short rate as in (8) and not the shadow rate.

[29]Note that for May 2014 we already use the DF rate that was introduced in June only, because, as argued in Section 2, the June rate cut and hence a switch to a new lower bound was largely already priced in in May.

the lower bound changes only once, i.e. $\hat{LB}_{AB} = 1$ bp and $\hat{LB}_C = $ -11 bps. Finally, the ATSM exceeds the likelihood of the SRTSM with ZLB, but the ATSM turns out to be dominated by all other shadow rate model specifications.

The preferred shadow-rate model specification that will be pursued throughout the remainder of the paper is SRTSM-2LB, with two lower bound regimes, $\hat{LB}_{AB} = 1$ bp and $\hat{LB}_C = $ -11 bps.

The complete set of model parameters corresponding to this specification is reported in Table 3 in the Appendix. Parameters correspond to the latent factors $\mathcal{P}_t$ rotated from the normalized latent factors X_t as in equation (21). For comparison, the ATSM parameters for similarly rotated latent factors $\mathcal{P}_t$ are reported in Table 4 in the Appendix.

As usual, factors are highly persistent for both models: under the $\mathbb{Q}$ measure, the highest eigenvalue of $(I + K_1^{\mathbb{Q}})$ exceeds 0.995 in both cases. However, under the $\mathbb{P}$ measure, the ATSM shows stronger mean reversion, with the highest eigenvalue of $(I + K_1^{\mathbb{P}})$ being 0.987 for the ATSM and 0.992 for the SRTSM-2LB. The standard deviation of the measurement error is estimated to be 3 bps, which indicates a close overall fit to the data. In line with the literature[30], parameters belonging to the $\mathbb{Q}$ dynamics are more precisely estimated than those belonging to $\mathbb{P}$ dynamics, as the former exploits at each point in time the full cross-section information. This pattern holds for both the SRTSM and the ATSM.

## 4.2 Estimated factors and shadow short rate

Given the estimated parameters, we back out the latent factors and the estimated shadow short rate using the standard (for the ATSM) or extended Kalman filter (for the SRTSM). As for the previous section, we focus on the latent factors $\mathcal{P}_t$ rotated from the normalized latent factors X_t using the loading matrix of observable principle components on observed yields, as described in Section 3.1. Not surprisingly, throughout the entire period, ATSM latent factors have the standard interpretation of 'level', 'slope' and 'curvature', as evident from the factor loadings, see Figure 7.[31] For the pre-low-rate period, also SRTSM factors have the interpretation of level, slope and curvature, as the loading profiles are qualitatively similar to those of the ATSM.

For the low-rate period, by contrast, the first factor from the ATSM and the SRTSM start to depart markedly from each other; see Figure 8. In fact, when the term structure is near the lower bound, there is no separate role for a level and a slope factor.[32] When short-term rates are stuck at the bound, any change at the long end of the curve is necessarily a change in the slope. A parallel shift of the curve – a movement that a typical level-factor shift would bring about – is a pattern which is essentially precluded from happening at the lower bound. Such a disappearance of a standard level factor is

---

[30]See, e.g., Bauer, Rudebusch, and Wu (2012), Kim and Orphanides (2012) or, more recently, Meldrum and Roberts-Sklar (2015).

[31]For the ATSM, these factor loadings are given by coefficients from equation (20) and are constant over time. For the SRTSM, there is no affine relation between factors and yields, and the loadings are computed instead as derivatives of yields with respect to factors. As the nonlinearity of the SRTSM implies that these depend on the current state and hence vary with time, loadings in Figure 7 are computed as averages of those derivatives over time.

[32]See also Kim and Priebsch (2013), who likewise discuss the disappearance of the level factor at the zero lower bound.
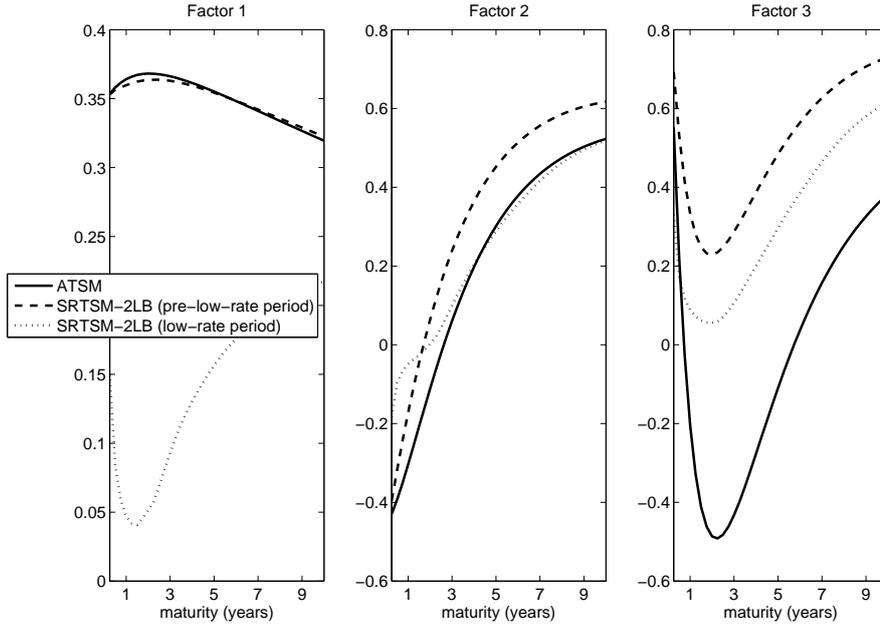
Figure 7: Loadings of fitted yields on factors.
Loadings of fitted yields (maturities from three-month to ten-year) on the three transformed latent pricing factors $\mathcal{P}_t$. For ATSM, loadings are coefficients $B_{\mathcal{P}}$ from equation (20), constant across the two sub-samples. For SRTSM-2LB, loadings depend on the level of factors, so the dashed (dotted) line represents average derivatives of fitted yields with respect to pricing factors $\mathcal{P}_t$ during the pre-low-rate (low-rate) period.

also found in our results. As the first element of $\rho_{1,\mathcal{P}}$ is positive (see Table 3) we know that an increase in the first factor increases the *shadow* rate. For the pre-low-rate period, this is tantamount to increasing the observable short rate (see Figure 7). For the low-rate period, by contrast, an increase of the first factor will only lead to an increase in the observable short rate if the shadow rate is sufficiently near the bound.

Furthermore, changes in the first factor lead to changes in expectations of the shadow rate, which in turn translate to a certain extent into changes of expectations of the short rate. The magnitude of these changes depends on the initial positioning of the expected shadow rate relative to the lower bound, see equation (5). Overall, the impact elasticity of the first factor on observable yields has become different from the pre-low-rate period. It no longer acts as a level factor, and its direct impact on the term structure as a whole has clearly diminished (see again Figure 7).

Regarding the shadow rate itself, the literature has pointed out that estimates of its position are highly sensitive to model specification and the quantification of the lower bound.[33] This is confirmed for our estimates for the euro area. Figure 9, upper panel, shows the estimated shadow short rates based on filtered factors for four model versions:

---

[33]See, e.g., the illustrations in Krippner (2015) and Bauer and Rudebusch (2016) for the U.S. and Christensen and Rudebusch (2015) for Japan. This in turn requires caution when giving specific economic interpretation to the shadow rate, e.g. as a measure for the monetary policy stance at times when the short rate is constrained by the lower bound, see, e.g., Krippner (2012) and Pericoli and Taboga (2015).
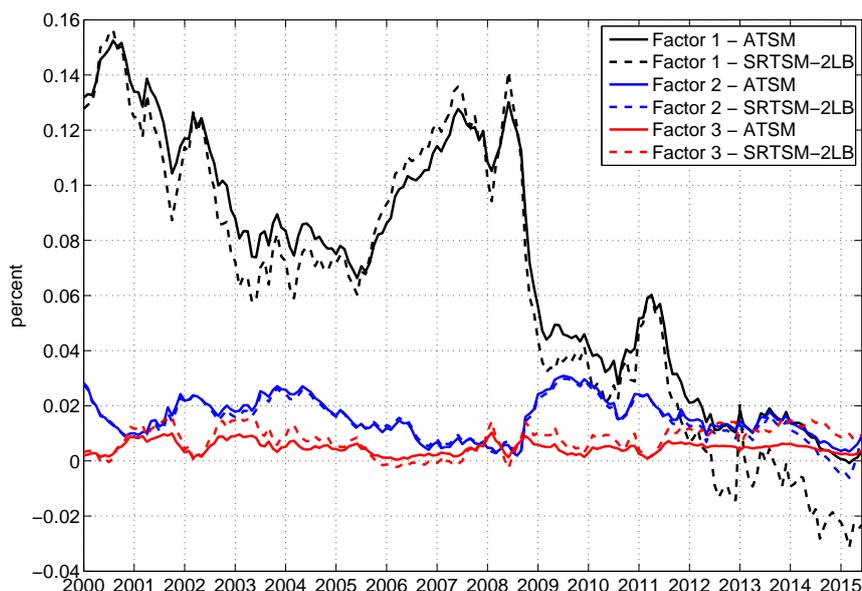
Figure 8: Filtered pricing factors.
The dashed (continuous) lines represent time-series of the three transformed latent factors $\mathcal{P}_t$ from SRTSM-2LB (ATSM), filtered with the extended (standard) Kalman filter.

the preferred model with two lower-bound regimes (SRTSM-2LB), the version with only one estimated lower bound (SRTSM-1LB), the version with a zero lower bound (SRTSM-ZLB), and the version with three different lower bound parameters set in accordance to the ECB's deposit facility rates (SRTSM-3LB-DFR).

The four versions of the model give rise to very different trajectories of the shadow short rate during the late low-rate period. The estimated shadow rate from the model with a zero lower bound stands out as reaching particularly deeply into negative territory. In order to understand this pattern, note that a model with a *zero* lower bound is clearly misspecified if spot and forward rates eventually wander consistently below zero. In such a situation, the SRTSM-ZLB can 'at best' match zero – the lowest attainable level – for current and expected future short rates, which the model engineers by putting current and expected shadow rates to deeply negative values so that $E_t(\max\{s_{t+h}, 0\}) = 0$.[34] The other three specifications imply less negative, yet still mutually different, shadow rate estimates.

As we consider multi-factor models, even when two models imply similar *level* esti-

---

[34]To illustrate the point, assume that the observed one-month forward rate h months ahead is -10 bps. An SRTSM with a zero lower bound will imply a fitted forward rate $f_t^h \approx \sigma_h^{\mathbb{Q}} \cdot H\left(\frac{\mu_{t,h}^{\mathbb{Q}} - LB - J_h}{\sigma_h^{\mathbb{Q}}}\right)$; see equation (12), which is by construction positive. That is, the fitted forward rate is even above the zero lower bound and hence the fitting error is above 10 bps. The SRTSM with a misspecified *zero* lower bound can minimize the misfit of the observed negative forward rate by decreasing the expected shadow short rate, $\mu_{t,h}^{\mathbb{Q}}$, which reduces $H(\cdot)$: for a very negative expected shadow rate, $\mu_{t,h}^{\mathbb{Q}} \ll 0$, $H(\cdot)$ converges to zero, so the model-implied forward rate converges to the zero lower bound and the misfit is minimized in the limit to 10 bps.

20
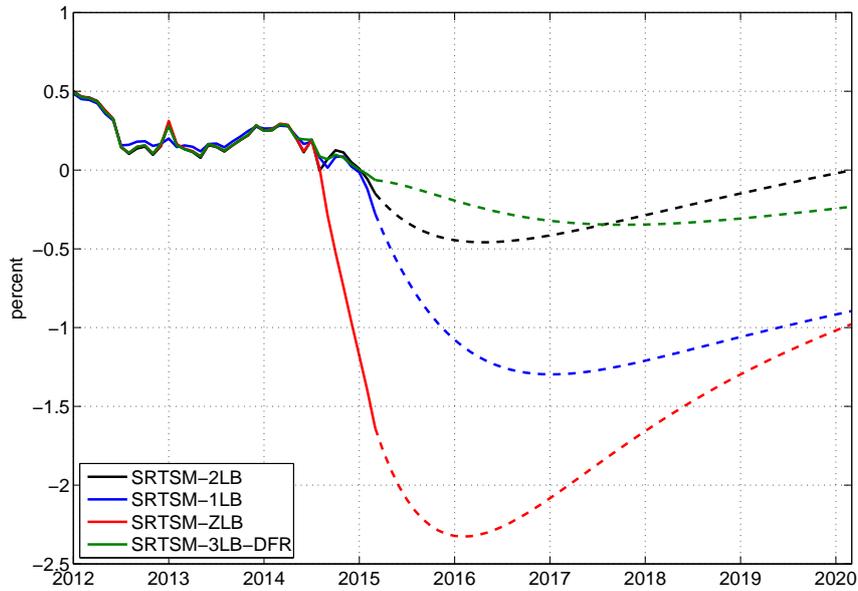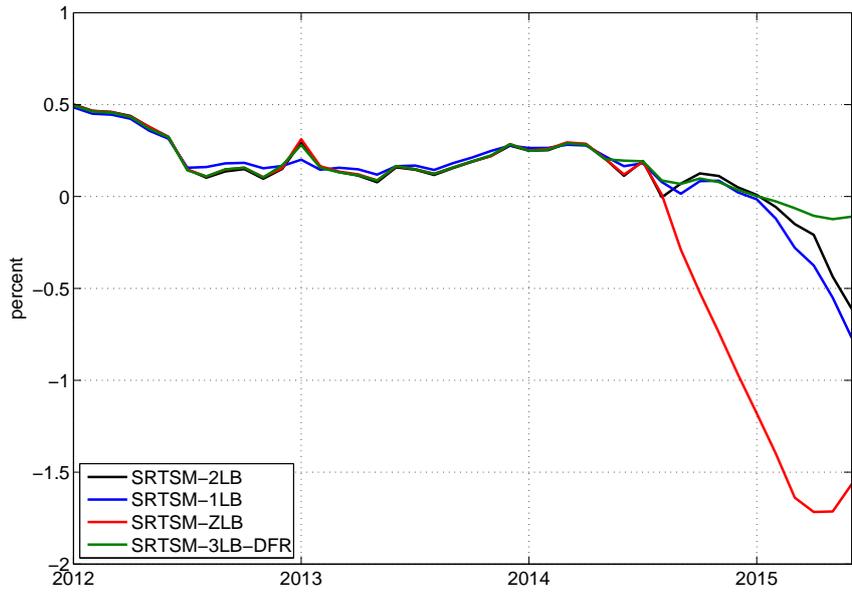
Figure 9: Shadow short rates: levels and expectations since 2012.
The upper panel shows monthly time-series of the filtered shadow short rate from four SRTSM
specifications from January 2012 to June 2015. The lower panel combines the same time series
up to March 2015 with conditional expectations at this date of future shadow short rates up to
five years ahead from all four SRTSMs.

mates of the shadow short rate, they may disagree about its *expected path* (see Figure 9, lower panel). As a case in point, note that our preferred SRTSM-2LB model and the model with one estimated lower bound, SRTSM-1LB, imply relatively similar shadow rate levels, but SRTSM-1LB features a much more persistent shadow-rate process. Accordingly, the shadow rate from that model is expected to stay at distinctly negative levels for a long time, so that farther-ahead expectations of short rates will range near the lower bound. As we will see further below, such differences in expected future shadow rates will translate into different estimated forward premia and different estimates of the time during which interest rates will stay below a certain threshold.

4.3 Goodness of fit and model-implied predictions

For both the pre-low-rate period (1999 to June 2012) and the low-rate period (July 2012 to June 2015), both the Gaussian model (ATSM) and the preferred shadow rate model specification (SRTSM-2LB) fit the yield curve on average very well (see Figure 10). The good fit is confirmed by the mean absolute error (MAE), which does not exceed 3 basis points for any maturity (see Table 5 in the Appendix). Overall, it is basically impossible to differentiate between the two models on the basis of in-sample fit.
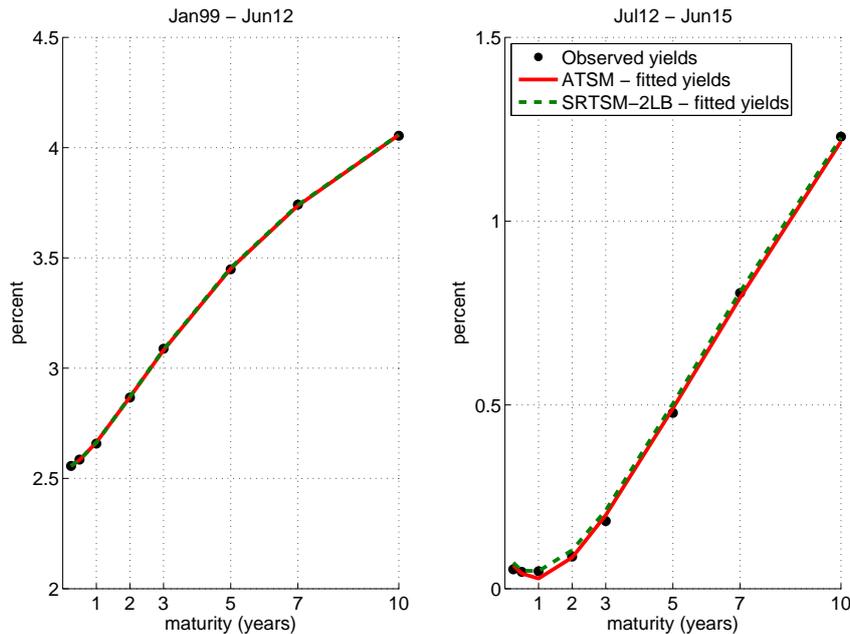
Figure 10: Average model-based fit of observed yields.
Average fitted yields from preferred specification SRTSM-2LB and the Gaussian ATSM together with average observed yields in the pre-low-rate period (left panel) and the low-rate period (right panel).

Despite providing a very similar in-sample fit to first moments, the *predictive* behavior of the two models can differ substantially during the low-rate period. In order to see why, recall that the Gaussian ATSM differs in two important dimensions from the shadow-rate models. On the one hand, the ATSM's mean reversion implies a relatively strong pull

back from low rates to the estimated long-run mean, contrary to the shadow rate model's 'sticking property' that can keep rates near the bound for an extended period of time. On the other hand, the short rate in the ATSM can assume arbitrarily low (and negative) levels, while short rates in the SRTSM have to obey the lower bound. And, indeed, both features can distinctly – and implausibly – shape the expected short rate path in the ATSM.

Regarding strong mean reversion, the lower panel of Figure 11 shows for April 2015 a strong tendency for the ATSM-implied short rate to quickly move up from the lower bound, while the SRTSM-2LB projects the short rate to stick near the bound for about one year still. As shown in the figure, the trajectory implied by the shadow-rate model is also more 'realistic' in the sense that survey expectations (derived from the ECB Survey of Professional Forecasters – SPF) saw a similarly sluggish upward creep of the short rate.[35]

Regarding the tendency of implausibly low ATSM rate projections, the upper panel of Figure 11 shows the ATSM-implied short-rate projection as of January 2014. While markets at that time were still assigning relatively little chance to negative rates, the ATSM projection took expected future rates distinctly below zero. This is different from the SRTSM-2LB, which is more in line with survey forecasts in seeing first a rather flat and then slightly rising rate evolution.

Apart from these two snapshots, on average the SRTSM-2LB also corresponds better to survey-based forecasts than the ATSM, both for a subsample starting in 2002 Q1[36] and ending in 2012 Q2, but especially in the low-rate period, see Table 6 in the Appendix.

Turning from first to second moments, Figure 12 compares the empirical volatility of one-year and three-year yields over a three-month horizon to its model-implied counterparts. For each month t, the empirical volatility of an n-month yield over an h-month horizon is computed by accounting for all daily changes of the yield in the H trading days of the following h months[37]

$$Vol_t^{Real}(y_{t+h}^n) = \sqrt{\sum_{i=1}^{H} \left(\Delta y_{t+i}^n\right)^2}. \tag{22}$$

For the ATSM, the corresponding model-implied conditional volatility has a closed-form expression given by:

$$Vol_t^{ATSM}(y_{t+h}^n) = \sqrt{Var_t(y_{t+h}^n)} = \sqrt{B_n' Var_t(X_{t+h}) B_n}, \tag{23}$$

---

[35]The comparison is complicated by the fact that survey participants are asked to express their views about future ECB MRO rates rather than future EONIA or OIS rates. In order to match model-implied forecasts with these surveys, we proceed as follows. In each quarter, at the survey's reply deadline date, we compute the 20-day backward average of the spread between EONIA and the MRO rate. While this spread was hovering around zero until end-2008, it turned sizeably negative as of 2009 Q2, i.e. the EONIA is below the MRO rate, which is due to the introduction of the ECB's fixed rate full allotment policy in late 2008. Accordingly, as of 2009 Q2, we subtract this spread from participants' average expectations of the future MRO rate in order to approximate the market view on the future short term money market rates.

[36]We choose this starting date as survey information about interest rates is not available earlier.

[37]See again Section 2 for more details on the daily data set used for computing the realized volatility.
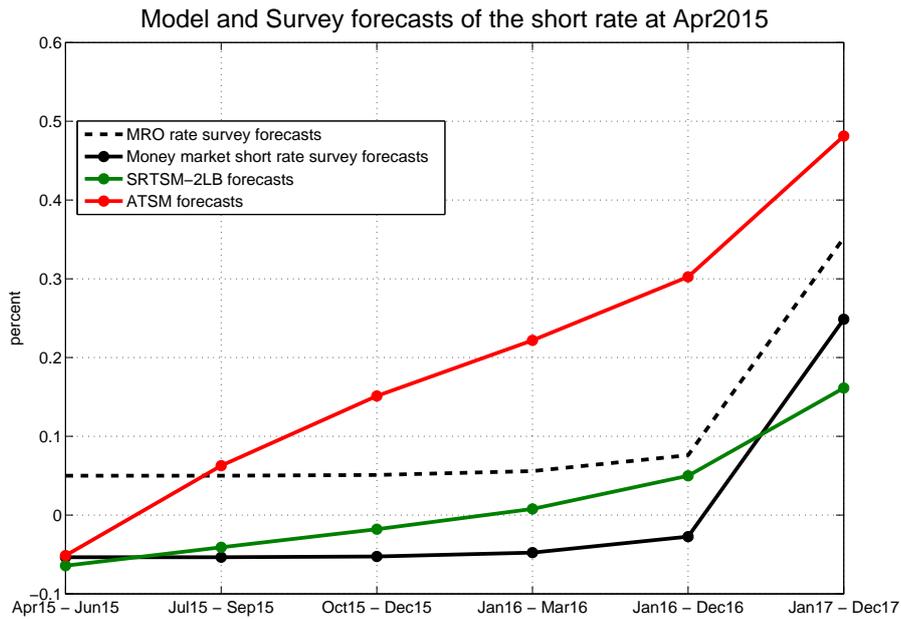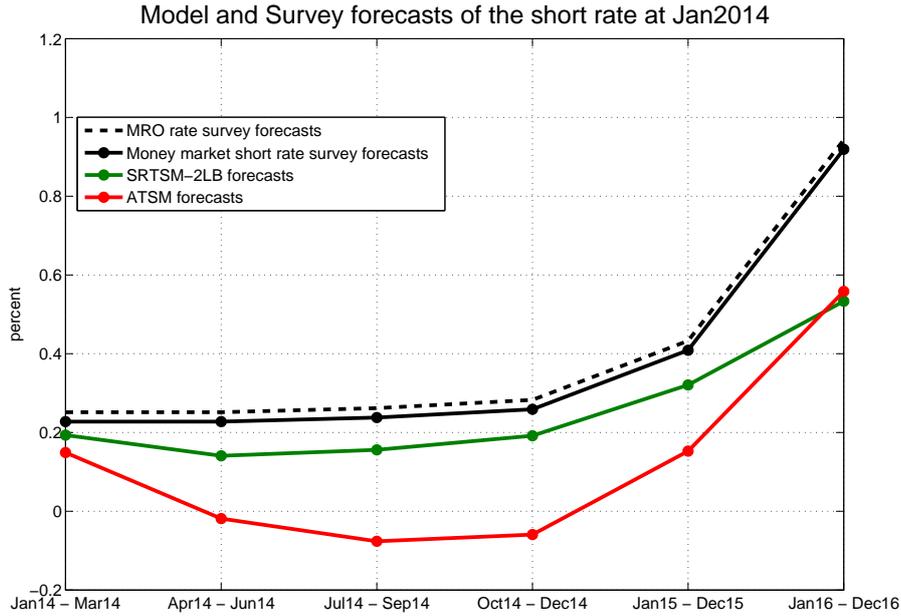
Figure 11: Models and survey expectations of future short rates.
Comparison of SRTSM-2LB and ATSM average ℙ-measure expectations of future short rates and survey average expectations of MRO rates from the ECB's Survey of Professional Forecasters (SPF). We approximate money market short rate survey expectations as MRO rate survey expectations adjusted for all forecast horizons with the 20-days moving average spread between EONIA and MRO rate prevailing at the date of the survey. The upper panel presents this comparison for January 2014 and the lower panel for April 2015. Forecast horizons are in line with SPF's framework: the current quarter, one quarter ahead, two quarters ahead, three quarters ahead, next calendar year, and calendar year after next. SPF panelists provide average MRO rate forecasts within each horizon, so we also average monthly forecasts across each horizon.

where $Var_t(X_{t+h})$ represents the conditional variance at time t of factors X for a horizon of h months. This variance is constant in the ATSM model, and hence, owing to the affine mapping from factors to yields, the conditional volatility of yields is also constant.

For shadow-rate models, by contrast, there is no analytical expression for the volatility $\sqrt{Var_t(y_{t+h}^n)}$, so we compute it based on simulation methods.[38] In the shadow-rate model, the volatility depends on the constellation of factors, and it tends to decrease with the level of the short rate. The intuition is that, whenever the shadow rate is far below the lower bound, the short rate is very likely to stay at the bound over short to medium horizons, so the volatility is lower than in normal times.

It turns out that the SRTSM-2LB traces the decline in volatility during the low-rate period quite well, while the ATSM over-estimates volatility during this period considerably (see Figure 12).
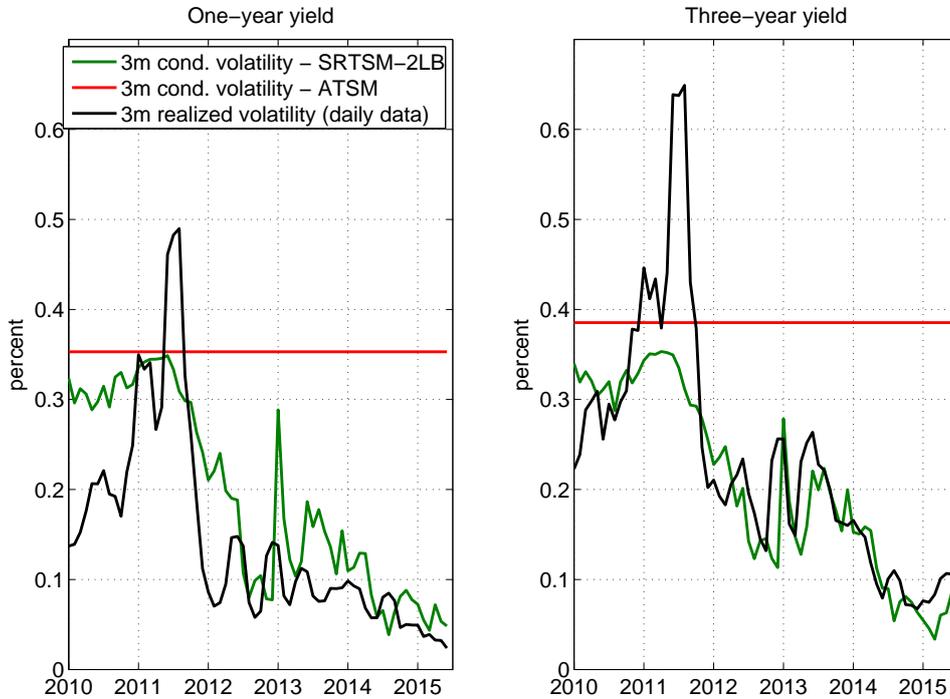
Figure 12: Three-month conditional volatilities of yields.
The left panel shows the time-varying three-month conditional volatility of the one-year yield from the SRTSM-2LB and the corresponding constant conditional volatility from the ATSM. Additionally, it shows the three-month realized volatility of the yield based on daily realizations. The right panel depicts the corresponding results for the three-month conditional volatility of the three-year yield.

---

[38]At each point in time t we compute the conditional Gaussian distribution of states X for future horizon h, i.e. we compute the conditional mean and variance of states based on the $\mathbb{P}$ parameters. We then draw 5,000 times from this distribution and for each draw we compute corresponding yields using (13). Finally, we compute the standard deviation of these 5,000 draws of yields.

4.4 Forward premia

As a further application, we use the estimated models to decompose the 1-month forward curve into expectations components and forward premia, respectively. One-month forward rates h periods ahead, f_t^h, are computed as:[39]

$$f_t^h = (h+1) \cdot y_t^{h+1} - h \cdot y_t^h \tag{24}$$

Forward premia fp_t^h are given as the difference between forward rates and the respective (physical) expectations of future short rates:

$$fp_t^h = f_t^h - E_t^{\mathbb{P}}(r_{t+h}) \tag{25}$$

As pointed out in the literature, fitting linear Gaussian models to the term structure when interest rates are near the lower bound leads to "implausibly large negative risk premiums" and tends to over-estimate their volatility.[40] For medium-term horizons, our results for the euro area go in the same direction, as shown in the lower panel of Figure 13. During the low-rate period, and especially since 2014, ATSM-implied three-year forward premia were uniformly more volatile and more negative than the respective measure derived from any of the shadow-rate model specifications. The intuition is again that the ATSM implies strong mean reversion so that expected future short rates return quickly to higher levels. Hence, at a time when markets expect rates to be persistently very low (as also suggested by surveys, as described above), the ATSM over-estimates expectations and under-estimates premia.

For short-term horizons, however, we document a different pattern. From 2012 to end-2014, the levels of ATSM-implied forward premia were *higher* than those of most shadow rate model specifications. This shows that over a short horizon, the property of the ATSM to assign high probabilities to implausibly negative levels of rates, which in turn leads to considerably smaller expectations, can dominate. As a case in point, consider again January 2014. While the preferred shadow-rate model and also surveys (see again Figure 11) projected a mildly positive short rate over the next six months, the ATSM predicted distinctly negative levels, hence unduly pushing up the forward premium.

Finally, while the difference in forward premia is most prominent in the comparison between the Gaussian model and the shadow-rate models, there are also differences among the different shadow-rate model specifications. Most strikingly, for the six-month horizon (top panel in Figure 13), forward premia for the SRTSM-ZLB specification are highest after late 2014 and essentially constant over time. This shows once more the problem of mis-specifying the lower bound as discussed before: at times of already negative rates, an inadequately chosen lower bound of zero forces the model's shadow rate to be very low and negative. This in turn implies that ($\mathbb{P}$) expected short-term rates are equal to zero for an extended period of time (see the straight line segment in the upper left panel of Figure 13). As $\mathbb{Q}$ expectations suffer from the same problem, forward premia are flat at zero as well. Regarding comparison between the other model specifications, the main take-away is that, even if the models imply similar shadow rate levels, their model-implied

---

[39]As usual, these are 'implied' forward rates: given the term structure of spot rates, they result directly from arbitrage considerations.

[40]See, in particular, Kim and Singleton (2012).
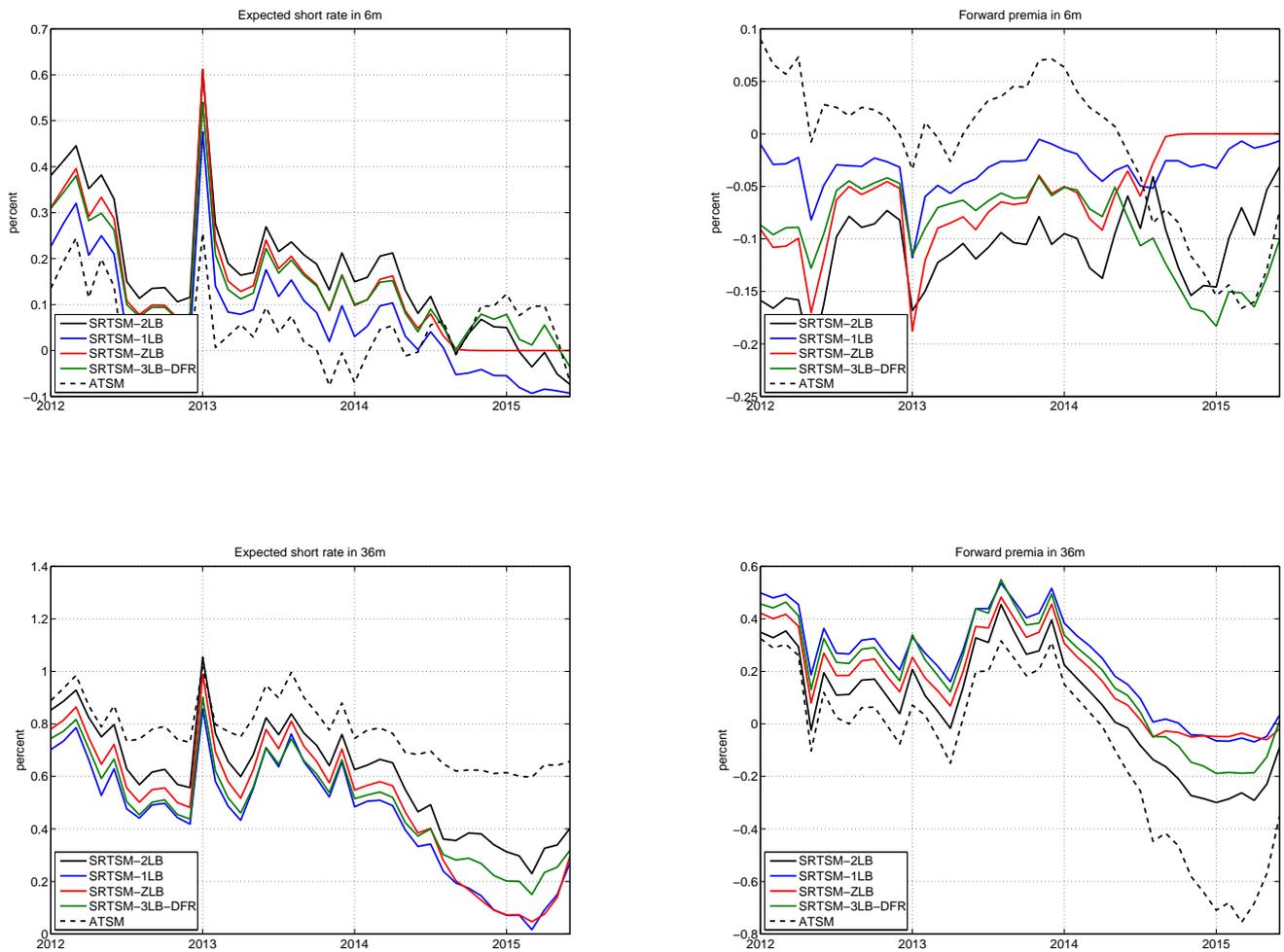
Figure 13: Forward rates decomposition into expectations and forward premia.
The upper panels shows the decomposition of the fitted one-month forward rates in six months (f_t^6) into the expectation component and the forward premium, as in equation (25), from four SRTSM specifications and the ATSM. The lower panels present the corresponding decompositions of the fitted one-month forward rates in three years (f_t^{36}) from the five models.

expectations and, hence, premia can differ distinctly. This is a consequence of the different degrees of estimated persistence across SRTSM specifications.

5   Timing the liftoff from the lower bound

When short-term interest rates are stuck near the lower bound, a shadow-rate term structure model can help to gauge how long it takes until rates will once again lift off from the bound.[41] For capturing the liftoff timing, the literature often resorts to the moment when future short-term interest rates will cross a certain threshold, usually set at a level somewhat above the lower bound. Using a fixed threshold instead of the lower bound itself makes especially good sense in our framework, where the lower bound is subject to change: fixing a threshold avoids 'spuriously' inferring a change in liftoff timing that stems purely from a changing bound.[42]

Specifically, we use the shadow-rate model to infer the timing when the short rate is expected to again cross the threshold of $c = 25$ bps, and then stay above that level for at least $K = 12$ months. Formally, we define at a given month t for any sequence of future short rates $\{r_{t+1}, r_{t+2}, \ldots\}$, for a threshold $c > r_t$ and for $K > 0$ the crossing time τ as $\tau = \min_{\tilde{\tau}}\{\tilde{\tau}|r_{t+s} > c,\ \text{for } s = \tilde{\tau}, \tilde{\tau} + 1, \ldots, \tilde{\tau} + K - 1\}$: that is, τ is the earliest point in the future, after which the short rate will stay above the threshold for at least K months.

Having an estimated term structure model at hand, one is able to construct the full distribution of such a crossing time via Monte Carlo simulation in a straightforward fashion. For given parameters and given factors at time t, one samples various (we take 10,000) short rate trajectories under the $\mathbb{P}$ measure. For each such path, one identifies the first crossing time as defined above and saves it. Hence, one ends up with 10,000 simulated crossing times, from which one computes moments, quantiles, etc. The median crossing time τ^* is then defined to satisfy $Prob(\tau < \tau^*) = 0.5$.

Using our preferred model, we illustrate in Figure 14 the conditional distribution of the timing when the threshold of 25 bps will be exceeded by the short rate based on information available in June 2015. The model suggests that the market's median timing to return to 25 bps is almost four years. However, the uncertainty around that number is relatively large, as the interquartile range goes from about two years to more than seven years. The distribution of the timing is asymmetric, as the liftoff timing is naturally bounded by zero, while it can also occur very late with positive probability.

In order to check the plausibility of the model-based liftoff results, they can be compared with a model-free approach based on the forward curve: as liftoff timing one would simply take the point in time when the forward curve[43] crosses 25 bps ('forward-curve-crossing heuristic'). And indeed, when the forward curve crosses the threshold, this is approximately[44] the time when the (risk-neutral) expected short rate jumps above that

---

[41]See especially the careful discussion in Bauer and Rudebusch (2016).

[42]As long as the bound is below the selected fixed threshold, a changing bound will not influence the liftoff timing. This is because the event of the short rate crossing the threshold is equivalent to the shadow short rate crossing the threshold and the distribution of future shadow rates is independent of the level of the lower bound.

[43]That is, the sequence of 1-month forward rates f_t^h, as defined in (24), for $h = 1, 2, \cdots$ plotted against horizon h.

[44]'Approximately', because the risk-neutral expected short rate differs from the forward rate by a
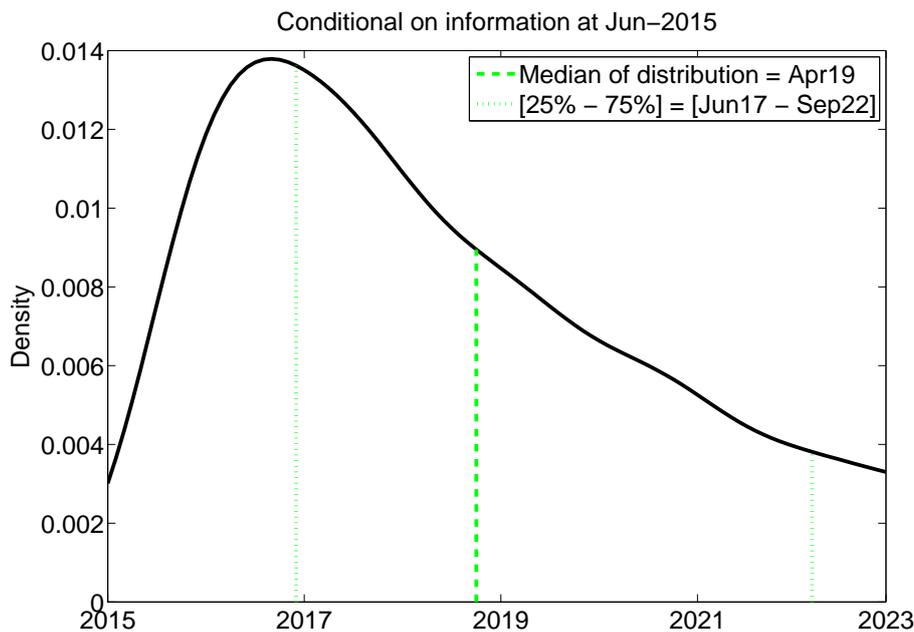
Figure 14: Conditional distribution of crossing time from SRTSM-2LB.
Distribution of the future moment when the short rate will exceed the threshold $c = 25$ bps, conditional on information in June 2015. The distribution is constructed by Monte Carlo simulation, recording for each simulated future path of the short rate constructed using $\mathbb{P}$-measure dynamics the moment when the path exceeds for the first time the threshold and stays above it for at least $K = 12$ months. See Section 5 for details.

level. However, this heuristic tends to give a biased metric of the true median crossing time for two reasons. First, as explained in Bauer and Rudebusch (2016), the distribution of the short rate near the bound is asymmetric. That is, at the time when the forward curve crosses the threshold, a considerable (risk-neutral) probability mass is assigned to the short rate being equal to the bound. This implies, in turn, that more than half of the possible short-rate trajectories are expected to cross the threshold *after* the crossing time derived from the forward-curve crossing heuristic. Second, as the forward curve reflects risk-neutral short-rate expectations rather than the real-world expectations, it does not reflect rate expectations as such, but rather rate expectations plus premia, as illustrated in Section 4.4 above.

The first feature (asymmetry) would suggest an *underestimation* of the liftoff time, while the second feature (premia) would suggest that the simple forward-curve-crossing metric *overestimates* the liftoff time if forward premia are negative.[45] Hence, as these two effects go in different directions, the simple forward-curve-crossing heuristic may possibly be not too bad an estimate of the true model-consistent median crossing time, to the extent that the two errors (ignoring asymmetry and ignoring premia) off-set each other.

Against this background, Figure 15 shows four potential measures of crossing time

---

(small) Jensen inequality term.

[45] Naturally, in case of positive forward premia the forward-curve-crossing metric would underestimate the liftoff time.

for a threshold set at $c = 25$ bps as of February 2013. First, the median crossing time derived with the simulation approach based on the SRTSM-2LB described above and using $\mathbb{P}$ dynamics of the short rate: assuming that the model is an adequate representation of term structure dynamics, this is the 'first-best' approach to capturing liftoff timing. Second, the simple heuristic based on the model-implied forward curve[46] crossing 25 bps: this would deviate from the first-best approach across two dimensions, namely by ignoring potential risk premia and the asymmetry of short rates near the bound. Third, the median crossing time derived from the preferred model, but this time using its $\mathbb{Q}$ dynamics: this variant helps to identify the effect of deviating from the first-best estimate by ignoring only premia, while taking into account asymmetry. And fourth, a similar approach as the forward-curve-heuristic, but replacing the forward curve by the model-implied $\mathbb{P}$-expected short rate path: this in turn takes into account possible premia, but ignores potential asymmetry. Finally, apart from those four lines representing point estimates of the crossing time, the figure shows the interquartile range (i.e. 25% to 75% quantile) implied by the SRTSM-2LB model as a shaded area, in order to gauge the uncertainty and skewness of the model-implied future liftoff time.
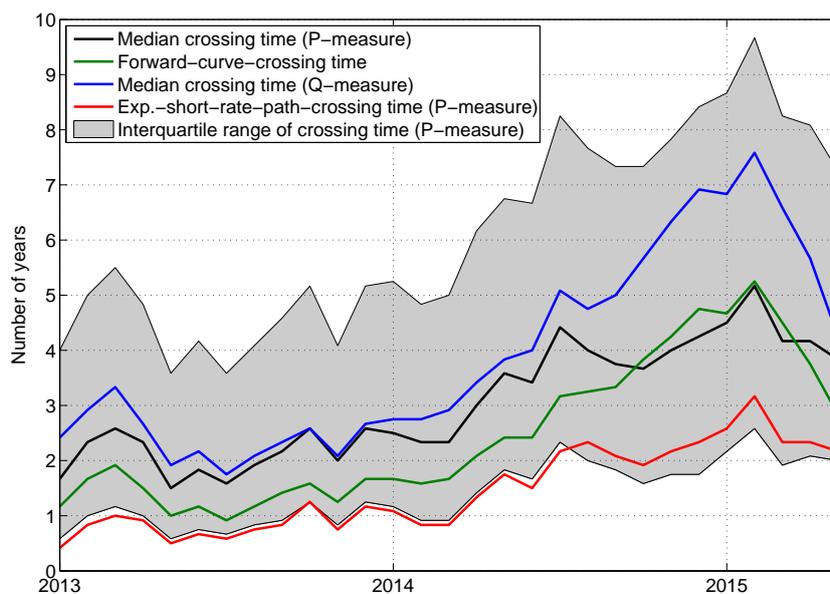
Figure 15: Indicators of liftoff from the lower bound from SRTSM-2LB.
Time-series of four measures of estimated liftoff timing from the preferred SRTSM-2LB: median crossing time constructed with $\mathbb{P}$- and $\mathbb{Q}$-measure dynamics of the short rate and crossing times based on the one-month forward curve and the $\mathbb{P}$-expected short rate path. The grey area represents the interquartile range of the median crossing time constructed with $\mathbb{P}$-measure dynamics of the short rate. All measures are constructed with a threshold of $c = 25$ bps, for February 2013 to June 2015.

As of February 2013, the model-implied $\mathbb{P}$-measure median crossing time ranges since

---

[46]Given the very good fit of the SRTSM-2LB model, the observed and model-implied forward curves are very similar.

February 2013 from 18 to 62 months. According to the model, the maximum duration was priced in by market participants in March 2015, when they were expecting low (smaller than 25 bps) interest rates to prevail for more than five years hence. The other three approaches deliver liftoff timings that occasionally differ significantly from the $\mathbb{P}$-measure median crossing time, despite exhibiting high correlation with this indicator. The forward-curve-crossing heuristic most closely resembles the model-implied median crossing time, especially since the end of 2014. This confirms the intuition that the effect of neglecting the asymmetry of interest rates in a lower-bound environment and the effect of neglecting the presence of negative forward premia partially compensate each other.

Our liftoff estimates are broadly in line with other studies focusing on the euro area. First, the preferred shadow-rate model specification in Kortela (2016), analyzing only risk-neutral indicators of euro-area liftoff timing, delivers a time series of the $\mathbb{Q}$-measure median crossing time that is very similar to our results for the $\mathbb{Q}$ measure. Second, the order of magnitude of our liftoff estimates are comparable to findings by Pericoli and Taboga (2015), who identify January 2020 as the first date of an increase in policy rates in the euro area conditional on information from January 2015.[47] At the same time, our maximum liftoff estimates of more than five years are longer than the maximum of three and a half years reported for the United States by Bauer and Rudebusch (2016), conditional on information from 2012.

Turning from the $\mathbb{P}$ median crossing time to its surrounding uncertainty, the shaded area in Figure 15 shows that the interquartile range of the model-implied crossing time distribution can be as wide as eight years. Moreover, this is only due to the shock uncertainty within the estimated model and does not take into account parameter uncertainty.

The uncertainty within a given model is of course confounded by uncertainty about the model itself. Figure 16 shows the $\mathbb{P}$-measure median crossing times from the four shadow-rate model variants. As of September 2014, we notice striking differences across models. Specifically, crossing times differ by more than four years between models with shifts in the lower bound (the preferred SRTSM-2LB and SRTSM-3LB-DFR) and those with a constant lower bound (SRTSM-1LB and SRTSM-ZLB). Note that the difference in crossing times is *not* monotonically related to the estimated *levels* of the shadow rates, but rather to their *persistence* (see again Figure 9): those models that feature a more persistent shadow rate, SRTSM-1LB and SRTSM-ZLB, also feature a longer $\mathbb{P}$-median crossing time.

6 The impact of a shifting lower bound

As discussed above, the decrease in the ECB's deposit facility rate in September 2014 was largely unexpected and may be interpreted to some extent as a negative 'shock' to the effective lower bound. Against this background, we use the shadow rate model to better understand the mechanics through which a decreasing lower bound LB can affect the term structure.

Consider, for instance, a situation where a zero lower bound prevails, and so the market excludes the possibility of negative rates. When the lower bound shifts down to, say, -20 bps, the market will start assigning positive probabilities to negative rates between zero

---

[47]The paper is not specific on whether these are results for the $\mathbb{Q}$ or the $\mathbb{P}$ measure.
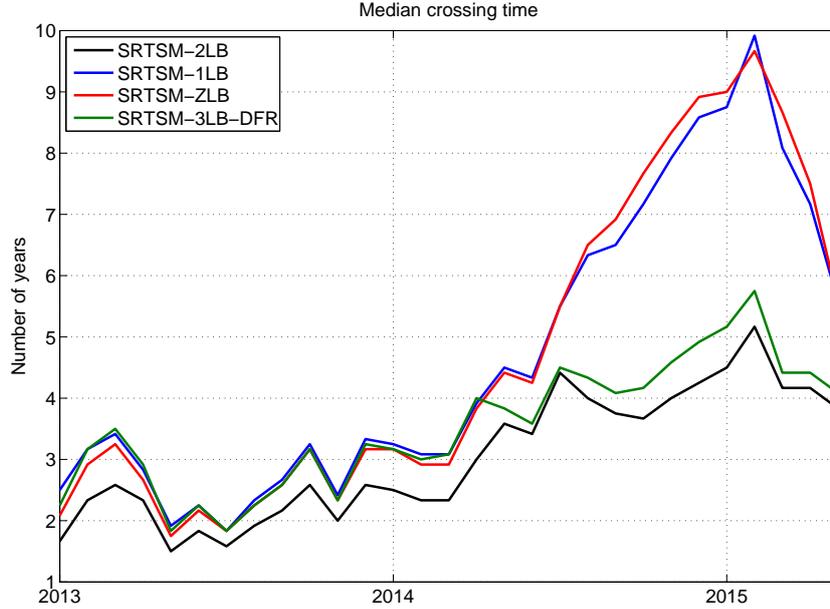
Figure 16: Comparison of median crossing time across SRTSM specifications.
Time-series of median crossing times from four SRSTM specifications, for February 2013 to June 2015. For comparability, all series are constructed with the simulation approach, a threshold of $c = 25$ bps and the $\mathbb{P}$-measure dynamics of short rates.

and -20 bps. That is, the conditional distribution of futures short rates expands to the left. This, in turn, decreases – *ceteris paribus* – expected short rates (under $\mathbb{P}$ and $\mathbb{Q}$ measure) and thus leads to declines in forward and spot rates.

More formally, recall from Section 3.1 that in the SRTSM the density of the shadow rate h periods ahead, conditional on information at time t, $p_t(s_{t+h})$, is Gaussian, while the conditional distribution of the short rate r_{t+h} has a censored normal distribution with a point mass of $Prob_t(s_{t+h} \leq LB)$ at LB and a normal density part $p_t(s_{t+h})$ to the right of it (see again Figure 6 for an illustration), both for the $\mathbb{P}$ and $\mathbb{Q}$ probability measure. If the lower bound is shifted down from LB to $LB - \delta$, $\delta > 0$, and assuming further that the distribution of the shadow rate $p_t(s_{t+h})$ is unaffected, the distribution of r_{t+h} changes in the following ways (see Figure 17): first, the interval $(LB - \delta, LB)$ is now being covered by non-zero probability after the shift; second, the point mass moves from LB to $LB - \delta$ and the point mass probability decreases (namely by the probability now assigned to rates falling into $(LB - \delta, LB)$); third, the density assigned to short rates above the old lower bound, i.e. in the interval (LB, ∞), remains unaffected.

Shifting down the lower bound leads unambiguously to a decrease of the expected short rate: taking the negative derivative of (5), and noting that $H'(x) = \Phi(x)$, one obtains, both for the $\mathbb{P}$ and $\mathbb{Q}$ probability measure, formula

$$-\frac{\partial E_t(r_{t+h})}{\partial LB} = \Phi\left(\frac{\mu_{t,h} - LB}{\sigma_h}\right) - 1, \tag{26}$$

32
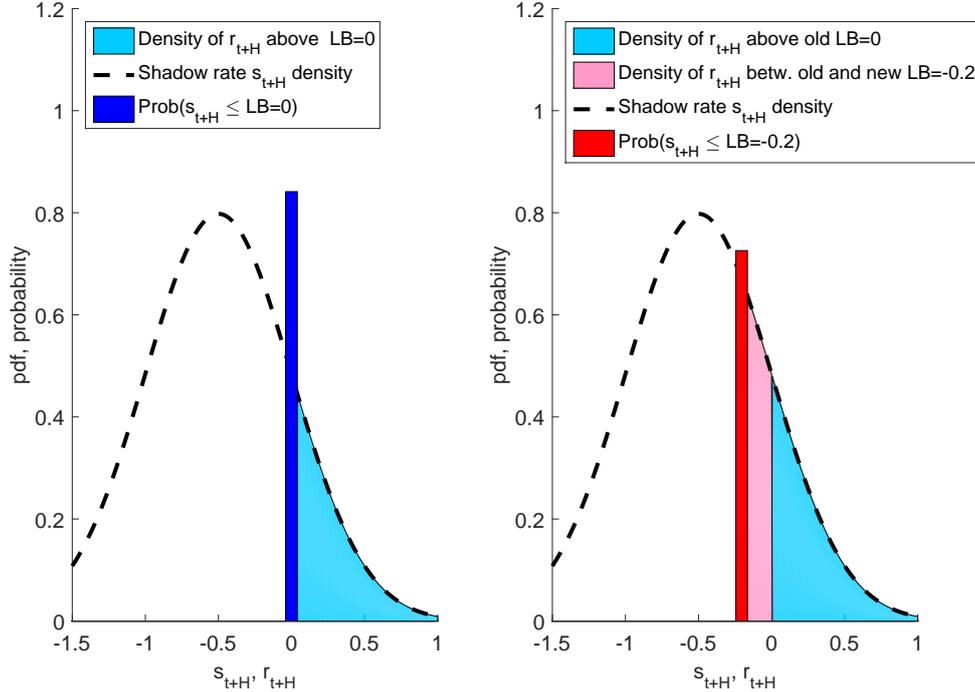
Figure 17: Illustration of the impact of a shift in the lower bound parameter on the predictive density of the short rate.
Left panel: Predictive distribution of short rate H months ahead, same as right panel in Figure 6. Arbitrary parametrization for illustrative purposes, lower bound $LB = 0$. Right panel: New predictive distribution of the short rate with same predictive shadow-rate density as in left panel, but lower bound shifted down to $LB = -0.2\%$. The new predictive distribution of the short rate consists of the point mass at the new lower bound (red) and the density part, which in turn consists of the part prevailing under the old bound (blue) and the new part (pink), indicating the feasibility of rates between the old and new lower bound, i.e. between 0 and -0.2%. Note that the difference between the point probability under the old LB and the new LB equals the area of the pink density part.

where $\mu_{t,h} = E_t(s_{t+h})$ and $\sigma_h = \sqrt{Var_t(s_{t+h})}$. This expression is clearly negative as $\Phi(\bullet) < 1$, i.e. a decrease in the lower bound leads – ceteris paribus – to decreased rate expectations. If $\mu_{t,h} \gg LB$, i.e. expected future shadow rates are far above the bound, then $\Phi \to 1$, i.e. a decrease in the bound has little effect on expected short rates. By contrast, if $\mu_{t,h} \ll LB$, i.e. expected shadow rates are far below the bound, then $\Phi \to 0$, i.e. a decrease in the bound shifts down expected rates almost one to one.

An analogous result holds for forward rates, where taking the negative derivative of (12) leads to

$$-\frac{\partial f_t^h}{\partial LB} = \Phi\left(\frac{E_t^{\mathbb{Q}}(s_{t+h}) - LB - J_h}{\sigma_h^{\mathbb{Q}}}\right) - 1, \tag{27}$$

i.e. the same expression as (26), but including the Jensen inequality term (which is independent of LB) as an additional argument. The interpretation is also the same: a decline in the lower bound leads to a decrease in the forward rate, and the effect is

stronger, the closer the forward rate is to the current lower bound. Figure 18 illustrates this by taking the negative derivative of the full forward and spot curve with respect to the lower bound at three different points in time. That is, for a specific month t, given SRTSM-2LB-estimated parameters and with a certain factor constellation in place, we apply (27) for horizons $h = 1, 2, \ldots$ to obtain the derivative of the forward curve. As spot rates are equal to average forward rates, the derivative of the n-month spot rate with respect to the lower bound parameter is the average of the derivatives of the respective forward rates.

In April 1999 (green lines), the yield curve was roughly equal to the average spot curve during the pre-low-rate period and rates were distant from the lower bound. Hence, a hypothetical shock to the lower bound would have hardly affected the term structure. In August 2014 (red lines), by contrast, rates were low, and current and expected shadow rates were below the bound up to distant horizons. Accordingly, a shock to the lower bound would affect the short end of the forward curve almost one to one, and still have a distinct impact even on longer maturities. Finally, June 2012 (blue lines) serves as an intermediate example. The observed forward and spot rates were already low but discernibly above the bound. Yet still, a shift in the bound is estimated to have a distinct impact on forward and spot rates, by expanding downwards the spectrum of rates that markets consider feasible, and thereby lowering expectations.

These results have an important implication for monetary policy: if the central bank manages to decrease the market's perceived location of the lower bound, it can thereby decrease forward and spot rates, even in a situation where the lower bound is not yet binding.

As an important qualification, we have assumed up to now in this section that the stipulated decrease in the lower bound is happening amid an unchanged constellation of current and expected shadow rates. This was done to single out more sharply the individual effect coming from a shifting bound. In reality, however, it is likely that any news that brings about a decrease in the lower bound will also affect current and expected risk factors (possibly to be interpreted as macroeconomic driving forces) and hence current and expected shadow rates.

This leads finally to the question, to what extent the shift in the yield curve between August and September 2014 is attributable to a pure shift in the effective lower bound and to what extent it is attributable to a shift in risk factors. Unfortunately, we cannot operate the model at daily frequency, so we cannot conduct anything close to an event study. Hence, our comparison of end-month snapshots needs to be interpreted as capturing all shocks happening over this time span, where the ECB rate cut of 4 September 2014 is just one event among several affecting yield curve factors, but arguably the only one that brought about the shift in the effective lower bound. Specifically, we decompose the total shift in the forward curve between end-August and end-September as follows: for each horizon h, denote by $f^h(\mathcal{P}^A; \Theta, LB^A)$, the model-implied 1-month forward rate for end-August, using the filtered factors $\mathcal{P}^A$, the lower bound $LB^A = 1$ bp and the other parameters Θ, and similarly by $f^h(\mathcal{P}^S; \Theta, LB^S)$ the model-implied forward rate for end-September at the new lower bound $LB = -11$ bps. We decompose the total change
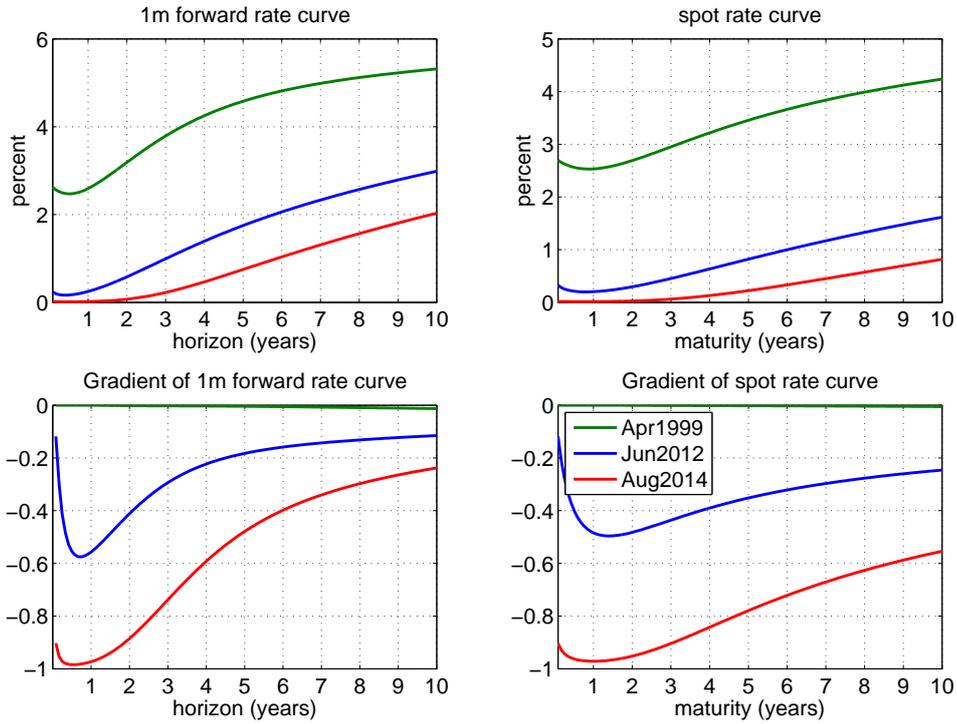
Figure 18: Impact of a shift in the lower bound parameter on forward and spot curves.
Top panel: one-month forward rate curves and term structures of zero-coupon rates for three selected dates: April 1999 (representative of the average spot curve in the pre-low-rate period), June 2012 (at end of the pre-low-rate period) and August 2014 (date before the lower bound shock). Lower panel: impact of an (infinitesimal) decrease of the lower bound on the one-month forward and zero-coupon rate curves on these selected dates.

$f^h(\mathcal{P}^S; \Theta, LB^S) - f^h(\mathcal{P}^A; \Theta, LB^A)$ as

$$
\begin{aligned}
& f^h(\mathcal{P}^S; \Theta, LB^S) - f^h(\mathcal{P}^A; \Theta, LB^A) \\
= & \underbrace{f^h(\mathcal{P}^S; \Theta, LB^S) - f^h(\mathcal{P}^A; \Theta, LB^S)}_{\text{Change in factors}} + \underbrace{f^h(\mathcal{P}^A; \Theta, LB^S) - f^h(\mathcal{P}^A; \Theta, LB^A)}_{\text{Change in lower bound}} \quad (28)
\end{aligned}
$$

Figure 19 shows the results. Until a horizon of about one year, the bulk of changes in the model-implied forward curve can be explained by the shift in the lower bound, while for longer horizons, changes in risk factors explain most of the changes in forward rates. However, in the absence of a macroeconomic underpinning, the model cannot shed light on the possible macroeconomic driving forces that are reflected by these changes in factors. The impact on the spot curve (not shown) is similar, with the lower-bound change having a somewhat more protracted effect also on higher maturities.
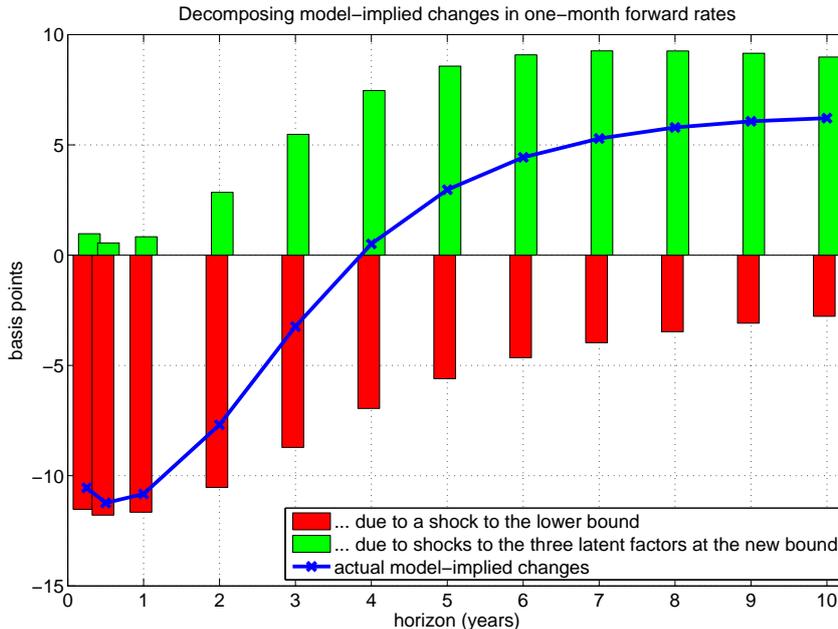
Figure 19: Decomposition of changes in one-month forward rates.
Decomposition of changes in fitted one-month forward rates from end-August to end-September 2014 into one component attributable to a decrease in the effective lower bound parameter and one attributable to changes in pricing factors.

7   Conclusion

We have estimated a shadow-rate term structure (SRTSM) model for the euro-area yield curve over the period from 1999 to June 2015. Model estimates identify an apparent shift in the market's perception of the effective lower bound from 1 bp (from 1999 to August 2014) to -11 bps (September 2014 to end of sample). The standard Gaussian affine model (ATSM), an SRTSM based on a constant *zero* lower bound assumption as well as a model with a constant estimated lower bound are rejected by the data. The SRTSM captures salient features of the term structure near the lower bound such as expected short rates sticking for long periods near the lower bound and a decrease in bond yield volatility. These properties cannot be captured by the ATSM. The model is also used to investigate the market-implied timing of liftoff from the lower bound (more precisely: when a threshold of 25 bps is again exceeded), which ranges from about one-and-a-half to five years during the low-rate period as of mid-2012. We also document that the quantification of the liftoff timing is highly dependent on the specification of the lower bound.

We also investigate analytically how a shift in the lower bound as such affects the yield curve. Hence, this comparative statics exercise treats the lower bound itself as a 'policy parameter'. We interpret the September 2014 drop in the euro-area OIS curve, following a largely unexpected ECB rate cut, from this perspective. We also show that an announcement of a decrease in the lower bound can decrease the yield curve even if the lower bound is not yet binding. This is because, ceteris paribus, the decreased

lower bound renders the distributions of future short rates less asymmetric and leads to assigning positive probabilities to rate realizations that had not been feasible under the old lower bound.

Our model allows for shifts in the lower bound at pre-set points in time. As shown in the paper, this specification is clearly preferred over one with a constant lower bound. As a natural extension, one could envisage a suitable (possibly discretely shifting) process for the lower bound. One would then also take a position on whether this would be a priced factor. Developing such ideas further is left for future research.

References

Akkaya, Y., R. Gürkaynak, B. Kısacıkoğlu, and J. Wright (2015). Forward guidance and asset prices. *IMES Discussion Paper Series E-6*.

Andreasen, M. M. and A. Meldrum (2015a). Dynamic term structure models: The best way to enforce the zero lower bound. *Bank of England Staff Working Paper 550*.

Andreasen, M. M. and A. Meldrum (2015b). Market beliefs about the UK monetary policy lift-off horizon: a no-arbitrage shadow rate term structure model approach. *Bank of England Staff Working Paper 541*.

Bauer, M. D. and G. D. Rudebusch (2016). Monetary policy expectations at the zero lower bound. *Forthcoming in Journal of Money, Credit and Banking*.

Bauer, M. D., G. D. Rudebusch, and J. C. Wu (2012). Correcting estimation bias in dynamic term structure models. *Journal of Business & Economic Statistics 30*(3), 454–467.

BIS (2005). Zero-coupon yield curve: technical documentation. *25*.

Black, F. (1995). Interest rates as options. *The Journal of Finance 50*(5), 1371–1376.

Bomfim, A. N. (2003). Interest rates as options: Assessing the markets' view of the liquidity trap. *Finance and Economics Discussion Series 45*.

Carriero, A., S. Mouabbi, and E. Vangelista (2015). UK term structure decompositions at the zero lower bound. *Queen Mary School of Economics and Finance Working Paper* (755).

Christensen, J. H. and G. D. Rudebusch (2015). Estimating shadow-rate term structure models with near-zero yields. *Journal of Financial Econometrics 13*(2), 226–259.

Christensen, J. H. and G. D. Rudebusch (2016). Modeling yields at the zero lower bound: Are shadow rates the solution? *Advances in Econometrics 35*, 75–125.

Cogley, T. and T. Sargent (2009). Anticipated utility and rational expectations as approximations of Bayesian decision making. *International Economic Review 49*, 185–221.

Damjanović, M. and I. Masten (2016). Shadow short rate and monetary policy in the euro area. *Empirica 43*, 279–298.

Duffie, D. and R. Kan (1996). A yield-factor model of interest rates. *Mathematical Finance 6*, 379–406.

ECB (2001). The Euro Money Market.

ECB (2014a). Euro area risk-free interest rates: Measurement issues, recent developments and relevance to monetary policy. In *Monthly Bulletin July 2014*, pp. 63–77.

ECB (2014b). Recent developments in excess liquidity and money market rates. In *Monthly Bulletin January 2014*, pp. 69–82.

Gorovoi, V. and V. Linetsky (2004). Black's model of interest rates as options, eigenfunction expansions and Japanese interest rates. *Mathematical Finance 14*(1), 49–78.

Greene, W. H. (1997). *Econometric Analysis* (3rd ed.). Prentice Hall.

Ichiue, H. and Y. Ueno (2006). Monetary policy and the yield curve at zero interest: The macro-finance model of interest rates as options. *Bank of Japan Working Paper Series E-16*.

Ichiue, H. and Y. Ueno (2007). Equilibrium interest rate and the yield curve in a low interest rate environment. *Bank of Japan Working Paper Series E-18*.

Ichiue, H. and Y. Ueno (2013). Estimating term premia at the zero bound: An analysis of Japanese, US, and UK yields. *Bank of Japan Working Paper Series E-8*.

Johannes, M., L. Lochstoer, and Y. Mou (2016). Learning about consumption dynamics. *Journal of Finance 71*(2), 551–600.

Joslin, S., K. J. Singleton, and H. Zhu (2011). A new perspective on Gaussian dynamic term structure models. *Review of Financial Studies 24*(3), 926–970.

Kim, D. H. and A. Orphanides (2012). Term structure estimation with survey data on interest rate forecasts. *Journal of Financial and Quantitative Analysis 47*(1), 241–272.

Kim, D. H. and M. Priebsch (2013). Estimation of multi-factor shadow-rate term structure models. mimeo.

Kim, D. H. and K. J. Singleton (2012). Term structure models and the zero bound: An empirical investigation of Japanese yields. *Journal of Econometrics 170*(1), 32–49.

Kortela, T. (2016). A shadow rate model with time-varying lower bound of interest rates. *Bank of Finland Research Discussion Paper 19*.

Krippner, L. (2012). Modifying Gaussian term structure models when interest rates are near the zero lower bound. *Reserve Bank of New Zealand Discussion Paper 02*.

Krippner, L. (2013a). A tractable framework for zero-lower-bound Gaussian term structure models. *CAMA Centre for Applied Macroeconomic Analysis Working Paper 49*.

Krippner, L. (2013b). Measuring the stance of monetary policy in zero lower bound environments. *Economics Letters 118*(1), 135–138.

Krippner, L. (2015). *Zero Lower Bound Term Structure Modeling: A Practitioner's Guide*. Palgrave-Macmillan.

Laubach, T., R. J. Tetlow, and J. C. Williams (2007). Learning and the Role of Macroeconomic Factors in the Term Structure of Interest Rates. mimeo.

Meldrum, A. and M. Roberts-Sklar (2015). Long-run priors for term structure models. *Bank of England Staff Working Paper 575*.

Monfort, A., F. Pegoraro, J.-P. Renne, and G. Roussellet (2015). Staying at zero with affine processes: A new dynamic term structure model. *Banque de France Document de Travail 558*.

Orphanides, A. and M. Wei (2012). Evolving macroeconomic perceptions and the term structure of interest rates. *Journal of Economic Dynamics and Control 36*(2), 239—-254.

Pericoli, M. and M. Taboga (2015). Understanding policy rates at the zero lower bound: insights from a Bayesian shadow rate model. *Bank d'Italia Working Papers 1023*.

Priebsch, M. (2013). Computing arbitrage-free yields in multi-factor Gaussian shadow-rate term structure models. *Finance and Economics Discussion Series 63*.

Ueno, Y., N. Baba, and Y. Sakurai (2006). The use of the Black model of interest rates as options for monitoring the JGB market expectations. *Bank of Japan Working Paper Series E-15*.

Wu, J. C. and F. D. Xia (2016). Measuring the macroeconomic impact of monetary policy at the zero lower bound. *Journal of Money, Credit, and Banking 48*(2-3), 253–291.

Yates, T. (2004). Monetary policy and the zero bound to interest rates: A review. *Journal of Economic Surveys 18*(3), 427–481.

Tables

Table 1: Summary of model specifications and their log-likelihoods

Nr.	Model name	Description	Log-likelihood
1	SRTSM-ZLB	$\hat{LB}_{ABC} = 0$ bps	9241.37
2	SRTSM-1LB	$\hat{LB}_{ABC} = -10$ bps	9350.89
3	SRTSM-2LB	$\hat{LB}_{AB} = 1$ bp, $\hat{LB}_C = -11$ bps	9375.89
4	SRTSM-3LB-DFR	$\hat{LB}_A = 0$ bps, $\hat{LB}_A = -10$ bps, $\hat{LB}_C = -20$ bps	9359.67
5	SRTSM-3LB	$\hat{LB}_A = 2$ bps, $\hat{LB}_A = 1$ bp, $\hat{LB}_C = -11$ bps	9377.13
6	ATSM		9303.05

The first five models – SRTSM – correspond to shadow rate term structure models with different lower bound parameter specifications across sub-periods: A – January 1999 to April 2014, B – May 2014 to August 2014, and C – September 2014 to June 2015. The sixth model – ATSM – is the Gaussian affine term structure model.

Table 2: Likelihood ratio tests

H_0	$logL_0$	H_1	$logL_1$	df	LR stats	p-value (%)
SRTSM-ZLB	9241.37	SRTSM-1LB	9350.89	1	219.04	0.0
SRTSM-1LB	9350.89	SRTSM-2LB	9375.89	1	50.00	0.0
SRTSM-2LB	9375.89	SRTSM-3LB	9377.13	1	2.49	11.5
SRTSM-3LB-DFR	9359.67	SRTSM-3LB	9377.13	3	34.93	0.0

The table shows four likelihood ratio tests for SRTSM specifications, going from the more parsimonious to the most flexible ones. The likelihood-ratio statistics are computed as $LR = -2 \cdot logL_0 + 2 \cdot logL_1$, where $logL_0$ and $logL_1$ are the log-likelihoods under the null and alternative, respectively. All log-likelihoods are conditional on $t = 1$.

Table 3: Parameter estimates of SRTSM-2LB

$K_{0,\mathcal{P}}^{\mathbb{Q}}$	-0.0009	0.0002	0.0003
	(0.0003)	(0.0002)	(0.0000)
$K_{1,\mathcal{P}}^{\mathbb{Q}}$	0.0019	0.1164	-0.0295
	(0.0003)	(0.0113)	(0.0491)
	-0.0036	-0.0396	0.1264
	(0.0001)	(0.0058)	(0.0261)
	0.0012	-0.0048	-0.0928
	(0.0000)	(0.0014)	(0.0066)
$\mathrm{eig}(K_{1,\mathcal{P}}^{\mathbb{Q}} + I(3))$	0.9961	0.9405	0.9329
$K_{0,\mathcal{P}}^{\mathbb{P}}$	0.0002	-0.0004	0.0008
	(0.0042)	(0.0013)	(0.0011)
$K_{1,\mathcal{P}}^{\mathbb{P}}$	-0.0152	0.0445	-0.0078
	(0.0114)	(0.1431)	(0.5277)
	0.0038	-0.0413	0.1023
	(0.0065)	(0.0449)	(0.0793)
	0.0025	-0.0077	-0.1206
	(0.0031)	(0.0437)	(0.1744)
$\mathrm{eig}(K_{1,\mathcal{P}}^{\mathbb{P}} + I(3))$	0.9915	0.9373	0.8942
$\Sigma_{\mathcal{P}}$	0.0066		
	(0.0009)		
	0.0000	0.0023	
	(0.0001)	(0.0002)	
	-0.0015	-0.0001	0.0012
	(0.0004)	(0.0002)	(0.0001)
$\rho_{1,\mathcal{P}}$	0.3499	-0.4499	0.8306
$\rho_{0,\mathcal{P}}$	-0.0015		
σ_e	0.0003		
	(0.0000)		
$\hat{LB}_{AB}$ (Jan1999 - Aug2014)	0.0001		
	(0.0001)		
$\hat{LB}_{C}$ (Sep2014 - Jun2015)	-0.0011		
	(0.0001)		

Maximum likelihood estimates of parameters of the SRTSM-2LB based on the extended Kalman filter, sample period January 1999 to June 2015. We report parameters for latent factors $\mathcal{P}_t$ rotated as in equation (21). Asymptotic standard errors are computed based on the inverse of the information matrix estimated using the first derivative of the likelihood function. As yields are measured in decimals (i.e. a yield of 3.5% would enter the data set as 0.035), the estimated standard deviation σ_e of the measurement error corresponds to 0.03% or 3 basis points.

Table 4: Parameter estimates of ATSM

$K_{0,\mathcal{P}}^{\mathbb{Q}}$	0.0006	-0.0005	0.0005
	(0.0000)	(0.0000)	(0.0000)
$K_{1,\mathcal{P}}^{\mathbb{Q}}$	0.0026	0.0638	-0.2446
	(0.0001)	(0.0005)	(0.0032)
	-0.0041	-0.0129	0.2373
	(0.0001)	(0.0005)	(0.0031)
	0.0013	-0.0110	-0.1188
	(0.0001)	(0.0005)	(0.0029)
$\text{eig}(K_{1,\mathcal{P}}^{\mathbb{Q}} + I(3))$	0.9958	0.9444	0.9307
$K_{0,\mathcal{P}}^{\mathbb{P}}$	0.0023	-0.0004	0.0004
	(0.0017)	(0.0009)	(0.0004)
$K_{1,\mathcal{P}}^{\mathbb{P}}$	-0.0033	0.0131	-0.5242
	(0.0106)	(0.0625)	(0.1946)
	-0.0010	-0.0435	0.2414
	(0.0050)	(0.0296)	(0.0807)
	0.0036	-0.0100	-0.1241
	(0.0025)	(0.0123)	(0.0430)
$\text{eig}(K_{1,\mathcal{P}}^{\mathbb{P}} + I(3))$	0.9874	0.9208	0.9208
$\Sigma_{\mathcal{P}}$	0.0048		
	(0.0003)		
	0.0005	0.0020	
	(0.0002)	(0.0001)	
	-0.0007	-0.0001	0.0008
	(0.0001)	(0.0001)	(0.0001)
$\rho_{1,\mathcal{P}}$	0.3499	-0.4499	0.8306
	(0.0002)	(0.0014)	(0.0088)
$\rho_{0,\mathcal{P}}$	-0.0015		
	(0.0000)		
σ_e	0.0003		
	(0.0000)		

Maximum likelihood estimates of parameters of the Gaussian ATSM based on the standard Kalman filter, sample period January 1999 to June 2015. We report parameters for latent factors $\mathcal{P}_t$ rotated as in equation (19). Asymptotic standard errors are computed based on the inverse of the information matrix estimated using the first derivative of the likelihood function.

Table 5: In-sample fit of models

Pre-low-rate period (January 1999 - June 2012)

MAE (bps)	Average	3m	6m	1y	2y	3y	5y	7y	10y
ATSM	**2**	2	2	3	1	3	2	1	2
SRTSM-2LB	**2**	2	2	3	2	3	2	1	2
Difference	**0**	0	0	0	0	0	0	0	0

Low-rate period (July 2012 - June 2015)

MAE (bps)	Average	3m	6m	1y	2y	3y	5y	7y	10y
ATSM	**2**	2	1	3	1	2	3	1	3
SRTSM-2LB	**2**	2	2	2	2	3	3	2	2
Difference	**0**	0	1	-1	1	1	0	1	-1

The upper panel shows mean absolute errors (MAE) of observed and fitted yields for the pre-low-rate period from the SRTSM-2LB and ATSM. Yields have maturities: one- and three-month, one-, two-, three-, five-, seven- and ten-year. Averages are computed across all eight maturities. All numbers in basis points. The lower panel shows the corresponding results for the low-rate-period.

Table 6: Model vs. survey expectations of future short rates

2002 Q1 - 2012 Q2

Forecast horizon	Avg.	Q0	Q1	Q2	Q3	Q4	Next calendar year	Calendar year after next
Number of observations		42	42	42	42	33	9	4
ATSM - MAE (bps)	**33**	22	24	27	32	35	57	9
SRTSM-2LB - MAE (bps)	**25**	21	18	21	26	33	49	9
Difference	**-8**	-1	-6	-7	-6	-2	-8	-1

2012 Q3 - 2015 Q3

Forecast horizon	Avg.	Q0	Q1	Q2	Q3	Q4	Next calendar year	Calendar year after next
Number of observations		13	13	13	14	-	13	13
ATSM - MAE (bps)	**30**	28	30	31	29	-	28	28
SRTSM-2LB - MAE (bps)	**20**	24	21	18	16	-	17	26
Difference	**-9**	-5	-10	-13	-13	-	-11	-2

Mean absolute error (MAE) of conditional average expectations of short rates from the ATSM and SRTSM-2LB vs. ECB Survey of Professional Forecasts (SPF) forecasts of average money market short rates. Survey forecasts are constructed from the SPF average MRO rate forecasts by subtracting the 20-days moving average spread between EONIA and the prevailing MRO rate at the deadline date of the survey, if this spread is negative (otherwise no spread correction). We match the closest end-of-month model-based conditional forecasts to each quarterly survey. The upper table covers the pre-low-rate period, starting however only in 2002 Q1, which was the first time that respondents' expectations for the MRO rate were reported. The lower panel shows the corresponding comparison for the low-rate period. Deviations of "Difference" are due to rounding.